

4. EQ PROGNOSTIC PARAMETERS DETERMINATION.

Seismologists consider the issue of “earthquake prediction”, as the “Holly Grail” of Seismology. In simple words, it is assumed as an impossible task. The reasoning, behind this notion, is clearly presented in Nature’s debate (moderator Ian Main, 1999) under the title “**Is the reliable prediction of individual earthquakes a realistic scientific goal?**”. The main objections (researcher, date), which are presented, against the possibility for a successful earthquake prediction methodology, are due to the following:

- **The Earth is a non-linear system:** Bowman and Samnis, 18-3-99; Sornette, 8-4-99; Main, 8-4-99.
- **The stochastic nature of earthquakes:** Wyss, 25-2-99; Scholz, 4-3-99; Geller, 11-3-99; Knopoff, 11-3-99; Bowman and Samnis, 18-3-99; Jackson, 18-3-99; Zhongliang Wu, 25-3-99; Crampin, 25-3-99; Wyss, 1-4-99.
- **Lack of physics theory of seismic source:** Geller, 25-2-99; Bernard, 11-3-99; Wyss, 11-3-99; Knopoff, 11-3-99; Sornette, 8-4-99; Main, 8-4-99.
- **Non-observable preparatory phase of earthquakes:** Wyss, 25-2-99; Bowman and Samnis, 18-3-99.
- **Doubts on existence and use of precursors:** Geller, 25-2-99; Michael, 4-3-99; Scholz, 4-3-99; Bak, 11-3-99; Bernard, 11-3-99; Knopoff, 11-3-99; Jackson, 18-3-99; Zhongliang Wu, 25-3-99; Main, 8-4-99.
- **Objections on methods, used, for earthquake prediction:** Geller, 25-2-99; Scholz, 4-3-99; Knopoff, 11-3-99; Jackson, 18-3-99; Bowman and Samnis, 18-3-99; Michael, 25-3-99;

Moreover, the question “Is the earthquake prediction possible?” has been answered in many different ways, ranging from “absolute negation” (Geller, 11-3-99) to “wonderful expectations” (Jackson, 18-3-99).

In the sections to follow, it will be shown that short-term earthquake prediction is possible, by integrating well-known laws of Physics / Geophysics to Earth geophysical models, which are in common use in routine geophysical targets to date. Consequently, the present work is not considered as a pure academic research project, but it should be treated rather, as a complicated, radically new, geophysical application.

The logical sequence, which evolves into a successful prediction, will be followed in the course of the presentation. At first we deal with **the parameter of time**. Then **the parameter of location** and **the magnitude parameter** will follow, which strictly depends on the first two.

4.1. Time of EQ occurrence determination.

After a strong earthquake has occurred at a seismogenic area, the immediate question which arises, is: when will it strike again? The seismologists worked out this question firstly because of its societal significance. This question implies, although in an indirect way, that the seismogenic area is already known and the, expected, magnitude of the future earthquake is almost similar, in magnitude, to the previous one or strong enough, so that it must be taken into account, seriously.

At the early steps of the scientific research for a successful earthquake prediction, the recurrence times of strong earthquakes, at a specific seismogenic area, were analyzed with statistical methods. The obtained, results refer to the long-term prediction, mainly. The fact that strong earthquakes are not very frequent prohibits, increased time resolution of the statistical methods which are used, due to the fact that the “sampling interval” is too long. A different statistical scheme, analyzes the **frequency – magnitude dependence and their logarithmic proportionality, the “b-value”** (Ma 1978, Smith 1986, Molchan et al. 1990) and variations of coda Q (Jin and Aki 1986, Sato 1986). Major earthquakes have been preceded by **seismic quiescence**. Kanamori (1981), Lay et al. (1982) Wyss et al. (1988) reviewed the methodology. Scholz (1988) studied the mechanisms, which could be responsible for this phenomenon, while Schreider (1990) proposed a statistical basis for making reliable predictions, based on quiescence. Gupta (2001) used the same methodology for the medium-term forecast of the 1988 northeast India earthquake.

As a result of this inability of the statistical methodologies to provide adequate time resolution (predictive time window for the future strong earthquake), which could be of some use for the society, different methodologies, more sophisticated, were developed. **The algorithm CN** is one of them (Keilis-Borok et al. 1990). This algorithm allows diagnosis of the times of increased probability of strong earthquakes (TIPs). The **CN** stands for the application of the TIPs methodology for California – Nevada, while a version addressed to magnitudes larger than $M=8R$ is assigned the name “**algorithm M8**” (Keilis-Borok and Kossobokov 1990; Romachkova et al. 1998).

Varnes (1989) studied the **accelerating release of seismic energy** or seismic moment either to time elapsed, or to time remaining, in the period preceding a main shock. He introduced empirical relations, having origins in both experiment and physical theory, going back many decades. The acceleration process was analyzed in laboratory experiments and was applied before strong earthquakes in Kamchatka and Italy by Di Giovambattista and Tyupkin (2001).

Narkunskaya and Shnirman (1990) proposed the **multiscale model of defect development**. Following this methodology and through simulation of the lithosphere, to a hierarchical discrete structure, which consists of some singularities, allows one to predict the time of appearance of “large” defects.

According to the **Load-Unload Response Ration (LURR) methodology**, when a system is stable, its response to loading corresponds to its response to unloading, whereas when the system approaches an unstable state, the response to loading and unloading becomes quite different (Yin et al. 1995, 1996, 2002).

Seismic quiescence and accelerating seismic energy release can be further detailed by the use of **the RTL algorithm**. This algorithm (Sobolev 2001, Sobolev et al. 2002, Di Giovambattista et al. 2004) analyze the RTL (Region, Time, Length) prognostic parameter, which is designed in such a way, to have a negative value if, in comparison with long-term background, there is a deficiency of events in the time – space vicinity of the tested area. The RTL parameter increases if activation of seismicity, takes place.

Seismicity “Pattern recognition algorithms” such as “ROC” – range of correlation – and “Accord” were used by Keilis-Borok (2002) to identify premonitory patterns of seismicity, months before strong earthquakes in Southern California. Another version of the pattern recognition methodology takes into account the earthquake intensities, in order to forecast the time of occurrence (Holliday et al. 2006).

In the **RTP (reverse tracing of precursors)** methodology, the precursors are considered in reverse order of their appearance (Keilis-Borok et al. 2004).

The methodology of **“Space-time ETAS”** (Ogata et al. 2006) is a further extension and improvement of the seismic quiescence methodology. ETAS stand for Epidemic Type Aftershock Sequence.

Yamashina (2006) used the **statistical test of time shift** for prediction studies in Japan.

The algorithm **SSE** (subsequent strong earthquake) was designed for prediction of relatively strong earthquakes following a strong earthquake. A subsequent, strong earthquake can be an aftershock or a main shock of larger magnitude.

The SSE algorithm resulted from the analysis of 21 case histories in California and Nevada. Then, it was, retrospectively, tested in 8 seismic regions of the world (Gvishiani et al. 1980, Levshina et al. 1992, Vorobieva et al. 1993, Vorobieva et al. 1994, Vorobieva 1994, Vorobieva 1999).

The statistical treatment of the earthquakes, which occurred at a specific seismogenic area in the past, has been proved more or less sufficient for the “medium-term or long-term” earthquake prediction. In terms of the “short-term” prediction the seismological literature has, not even a successful case, to present at all. Apart from the long time sampling interval, which elapses between two consecutive strong earthquakes in the same seismogenic area, there is an intrinsic difficulty in using statistical methods towards a successful, short-term earthquake prediction. This is analyzed as follows.

4.1.1. The mass - friction interaction model.

Any seismic event can be simulated by the following model, presented, in figure (4.1.1.1), and introduced, by Shimazaki and Nagata (1980). A mass, standing on the surface of a media, is pulled by a spring. As long as the pulling force (**e**), which is applied on the mass through the spring, is less than friction (**τ**) that exists between the mass and the media surface, the mass does not move. Consequently, each time there is inequality between friction and the pulling force (**e**) that is:

$$\tau \leq e \quad (4.1.1.1)$$

then, the mass starts moving and therefore due to the fact that the spring becomes shorter, the previous equation turns into the inequality:

$$\tau > e \quad (4.1.1.2)$$

This is graphically, presented, in the following figure (4.1.1.1).

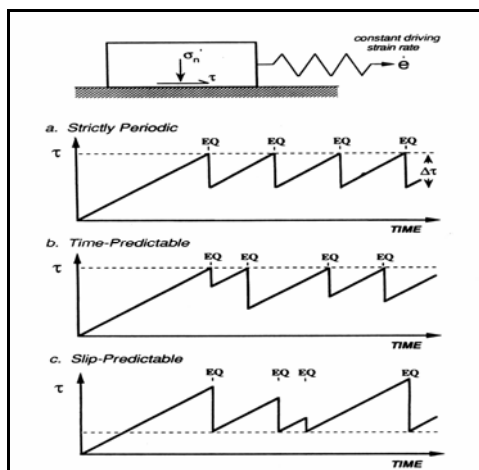


Fig. 4.1.1.1. The spring (mass-friction) model introduced, by Shimazaki and Nakata (1980).

A seismogenic area behaves in a similar way and in a first approximation. The seismogenic area is stress-strain, charged, for a time period (**fig. 4.1.1.1a**), until it reaches the critical, fracturing, stress-strain level. At this time, an earthquake (EQ) takes place and the overall, stress-strain load discharges (at Δt) to a lower level. If we assume that the critical, fracturing level and the discharge level are constant, then the recurrence time period of a strong EQ is determined by the time interval which elapsed between two consecutive EQs. This mode of recurrence time periods is called “**strictly periodic**”. This mode of charge – discharge procedure of a seismogenic area is just a theoretical approximation and does not reflect what is observed in nature.

Next model (**fig. 4.1.1.1.b**) assumes that the stress-strain charge is released through EQs of variable magnitudes (**time predictable**) to different final lower levels.

As an immediate result of this mode of energy release in a seismogenic area, different recurrence EQs times are observed. This is very common in the seismic activity, observed, in a specific seismogenic area. Consequently, a strong difficulty is imposed on any statistical analysis of the recurrence times of these EQs.

A third adopted model (**slip predictable**), is the one, presented, in figure (**4.1.1.1c**). In this case, the fracturing, stress-strain level is variable, while the lower, stress-strain discharge level is accepted as constant. Also, this model justifies the variable recurrence times of earthquakes in the same seismogenic region and implies the very same difficulties in the statistical determination of the recurrence time of these EQs.

Both models, “time predictable” and “slip predictable”, suggest the inability to apply statistical tests for the short-term prediction.

Moreover, it is not yet clear in nature which model is valid, each time a strong EQ is pending in a seismogenic region. Therefore, a more generalized model is postulated, in which both the “stress-strain” fracturing level, as well as the lower “discharge level”, are considered variable. This model is presented in the following figure (**4.1.1.2**).

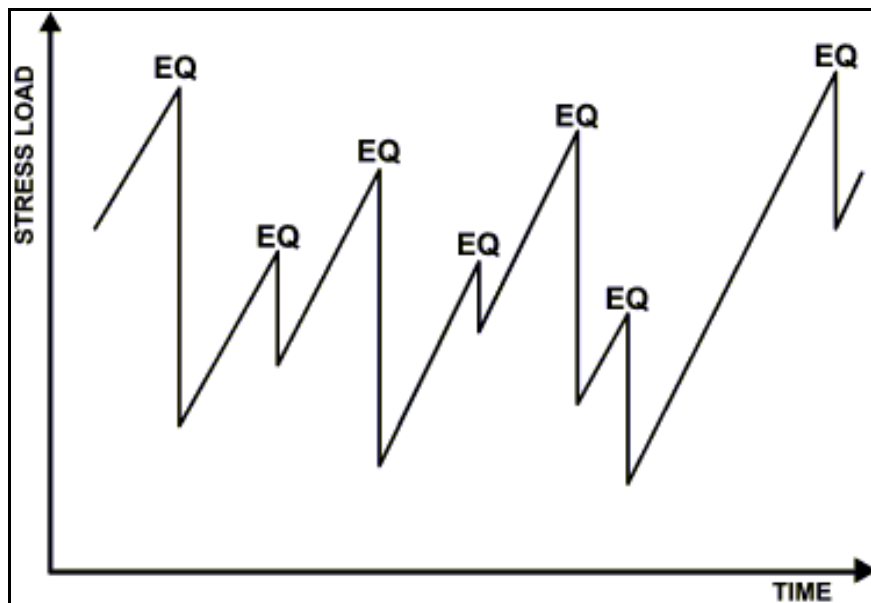


Fig. 4.1.1.2. A more generalized model of a seismogenic area in which both the “stress-strain” fracturing level, as well as the lower “discharge level”, are considered variable.

The introduction of variability in both, the stress-strain fracturing level as well as to the lower discharge level complicates much more the problem of studying the recurrence time of strong EQs.

Finally, the small magnitude random seismicity, which takes place in the time period which elapses in between two strong earthquakes, modifies the overall time T which is expected to elapse between them (Hori and Oike, 1999). This is explained by the following figure (**4.1.1.3**).

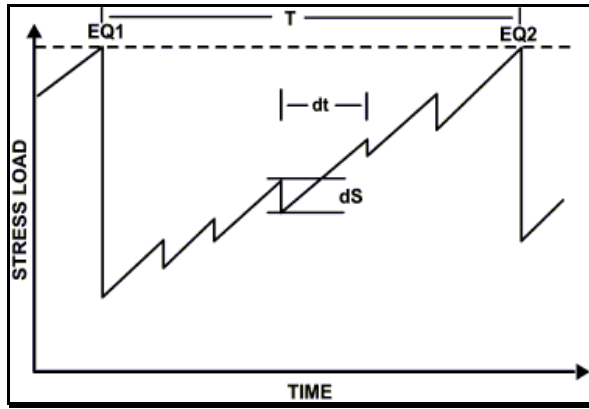


Fig. 4.1.1.3. Modification of time T , elapsed, between EQ1 and EQ2, due to small size seismicity which occurred in the same period of time in a specific seismogenic area, due to its small size seismicity (Hori and Oike, 1999).

What is interesting, in this mechanism, is the fact that, each time when a small earthquake occurs, the seismogenic area is, slightly (dS), stress-strain, discharged and therefore, it takes some time:

$$\Delta t = dS / (dS/dt). \quad (4.1.1.3)$$

Where:

Δt is the time, needed, by the seismogenic area, in order to recover to its previous charge state.

dS is the temporary stress-strain discharge, due to small size seismicity

dS/dT is the rate of stress-strain change of the seismogenic area, during this time period.

to recharge up to the previous state of stress – strain level.

Consequently, the overall time period T , between two consecutive, strong earthquakes, depends on the small size seismicity of the seismogenic area itself, too.

So far, all these models suggest a chaotic behavior of the seismogenic area, in terms of the time of occurrence of a strong EQ. This chaotic behavior of the seismogenic area, justifies what the seismologists accept as inability to predict a strong EQ in “short-term time”.

This unsolvable problem can be formulated, as follows, in a simple mathematical approach:

Let us assume that, before a strong EQ, the stress-strain charge of the seismogenic area is represented by a linear function:

$$S = at + b \quad (4.1.1.4)$$

Where (S) is the total stress-strain charge at a time (t), (a) represents the value dS/dt , (b) is a constant, while (S_{fr}) is the fracturing level (fig.4.1.1.4).

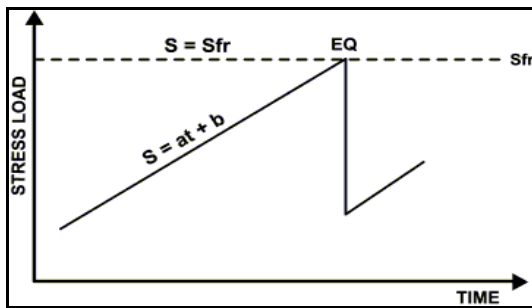


Fig. 4.1.1.4. The adopted, simplified model indicates the mathematical relation of the stress-strain charge, as a function of time, to the fracturing level of the seismogenic area.

Following these annotations, an earthquake occurs when at a certain time (t) both equations:

$$S = at + b \quad \text{and} \quad S = S_{fr} \quad (4.1.1.5)$$

are satisfied.

In the case of equations (4.1.1.4), the parameters (a), (b) and (Sfr) for a seismogenic area and for a certain time period (T), are unknown. Therefore, the time (to) for the occurrence of a strong EQ can be determined, only, after having assigned arbitrary values on the parameters of equations, present in (4.1.1.5). **In mathematical terms, this suggests that the system of equations (4.1.1.5) is undefined and therefore, there is an infinite number of solutions, referring to (to), the time of occurrence of the future, strong EQ.**

The space of solutions of equations (4.1.1.5) incorporates a) arbitrary solutions in (to), which have no seismological significance (in terms of stress-strain charge status of the seismogenic region) and b) true solutions in (to), which are closely related to the real strong earthquakes which will take place at the (to) time in the future. Therefore, the real “time prediction problem” is to find a way to distinguish the (b) type solutions of equations (4.1.1.5), from the infinite space of its arbitrary solutions.

The statistical schemes, which are used to date, have been proved unsuccessful to this end. In contrast to the used statistics, the solutions of equations (4.1.1.5) will be constrained by the use of a specific physical model, namely “the lithospheric oscillating plate”, which was presented in section (2.5.2). In practice, the “AND” operator of the Boolean algebra, is used between the solutions of the equations (4.1.1.5) and the solutions which result from the use of the lithospheric, oscillating plate model.

The stress charge in the future EQ focal area is due to two stress-increasing mechanisms:

The first one is the plate’s motion. The motion of the local lithospheric plates is the most important factor in stress increase in a specific seismic area. The following figure (4.1.1.5) presents the tectonic plate’s model, which holds for the Aegean area, Greece (McKenzie 1972, 1978).

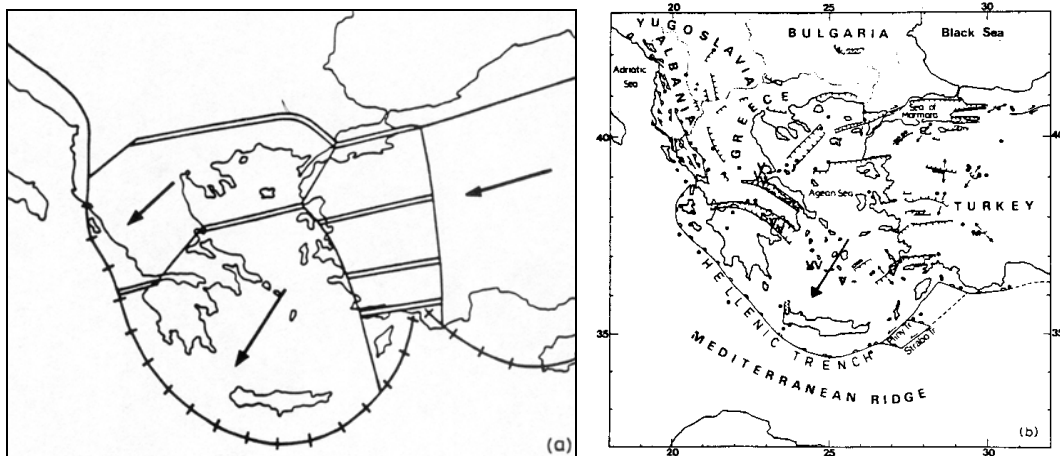


Fig. 4.1.1.5. The Aegean area, plate models proposed, by McKenzie (a - 1972, b - 1978).

The kinematics of the same area was studied by Papazachos et al. (1996). The active, crustal deformation in the Aegean and the surrounding area appear in the following figure (4.1.1.6).

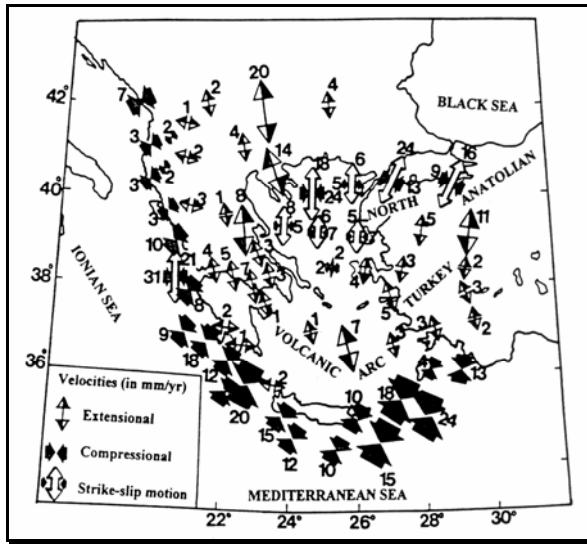


Fig. 4.1.1.6. Plate kinematics and crustal deformation in the Aegean area (after Papazachos et al., 1996)

The second one is the lithospheric plate oscillation, as it was briefly presented in section (2.5.2). The influence of the tidal forces upon the Earth's surface and their effect, as a triggering mechanism upon the generation of earthquakes, had been also studied by Tamrazyan (1967, 1968), Liu et al. (1985), Shirley (1988), Bragin et al. (1999), Thanassoulas et al. (2001a, b), Duma et al. (2003), Tanaka et al. (2006).

In this section, a more detailed analysis will be presented, as far as it concerns the way the tidal forces affect the stress-strain charge status of a seismogenic area which is considered as subjected to tidal forces (**T**).

4.1.2 Tidal forces acting upon the lithosphere.

The tidal forces (**T**) which are applied on the lithosphere (**fig. 4.1.2.1**) are decomposed into two components: a) the horizontal (**T_x**), and b) the normal (**T_z**), to the lithospheric plate.

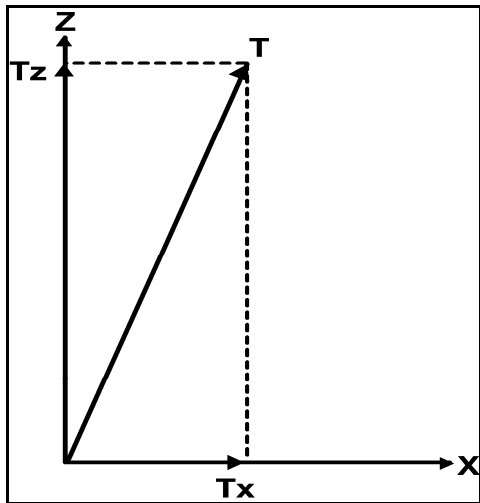


Fig. 4.1.2.1. Analysis of the tidal force (**T**) into its horizontal (**T_x**) and vertical (**T_z**) components.

Furthermore, the (**T_x**) component can be analyzed into its horizontal subcomponents, related, to the strike of the existing fault in the seismogenic area. Therefore, assuming that:

$$T_v = T_x \quad (4.1.2.1)$$

The orthogonal analysis of (**T_v**) into two axes, one normal to the fault strike and the other along it, results into the horizontal tidal forces components of **T_{al}** (along the fault strike) and **T_{nm}** (normal to fault strike), presented, in the following figure (**4.1.2.2**).

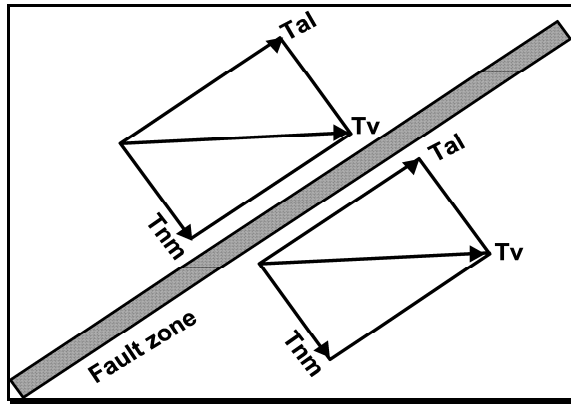


Fig. 4.1.2.2. Analysis of the horizontal (T_v) component of the tidal force, into two orthogonal components (T_{al} , T_{nm}), along and normal to the seismogenic fault strike.

The horizontal tidal component (T_v) is the same (in amplitude and direction), in both sides of the seismogenic fault. Consequently, no stress-strain increase or decrease can develop in the fault zone which in turn will modify its overall stress-strain charge.

On the contrary to the horizontal component, the normal one (T_z) to the lithospheric plate will force it to oscillate in the same frequency spectrum, as the tidal forces oscillate. A sketch drawing of the oscillating lithospheric plate is presented in fig. (4.1.2.3).

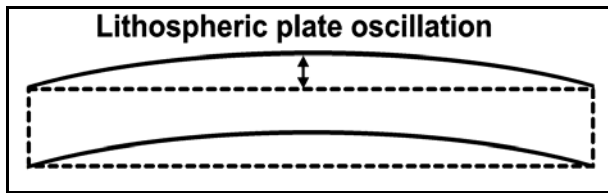


Fig. 4.1.2.3. The lithospheric plate oscillates, triggered by the oscillating tidal forces. The dotted rectangle is the lithosphere at its rest position, while the solid, curved rectangle represents the oscillating lithosphere. Double arrow indicates the oscillation amplitude.

The lithospheric oscillation has a significant consequence. The length of the part of the lithospheric plate that oscillates, changes, due to its oscillatory deformation. This is presented in the following figure (4.1.2.4).

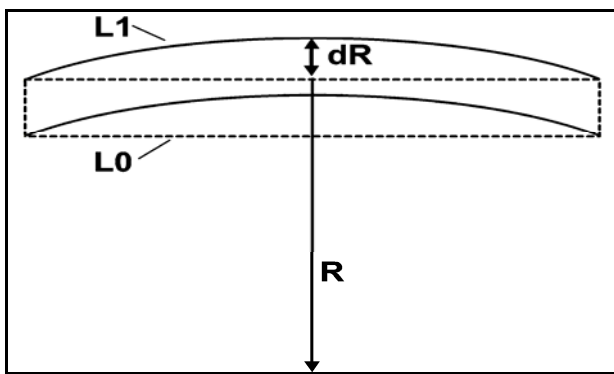


Fig. 4.1.2.4. Change of length L_0 of lithosphere into L_1 , due to its oscillation.

Moreover, the oscillating lithospheric plate increases its distance from the Earth's center at (dR), where (R) is the radius of the Earth at the seismogenic area. By denoting as (φ) the angle, which is defined by the oscillating lithospheric plate (arc) and the center of the Earth (fig. 4.1.2.5), then the following equation holds:

$$dL = \varphi \cdot dR \quad (4.1.2.2)$$

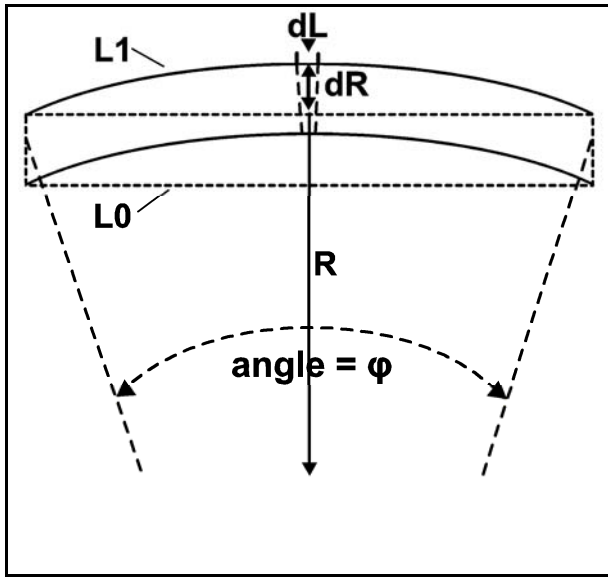


Fig. 4.1.2.5. Sketch drawing that indicates the deforming mechanism of the oscillating lithospheric plate.

By taking into account that (dR) is an oscillating parameter, due to tidal forces and the strain definition (Jaeger, 1974) of (ϵ) as:

$$\epsilon = dL/L \quad (4.1.2.3)$$

and by combining (4.1.1.2) with (4.1.2.3), it results into an oscillatory strain (ϵ) component, with its maximum effect, applied, at the center of the plate. Therefore, for a monochromatic lithospheric oscillation, the strain will have the form:

$$\epsilon = \epsilon_0 \cdot \sin(2\pi T^{-1}t) \quad (4.1.2.4)$$

where: (T) is the period of oscillation.

The oscillatory strain, represented by equation (4.1.2.4), generates the corresponding compressional and extensional forces S (fig. 4.1.2.6), required, to trigger an earthquake, in any fault that is close to rupture.

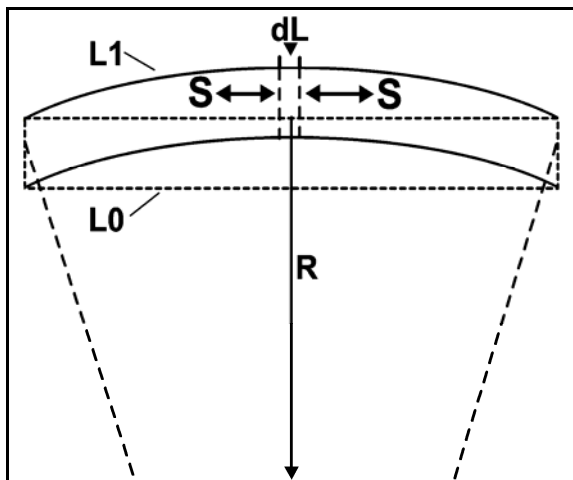


Fig. 4.1.2.6. Compressional and extensional oscillatory forces (S), generated, in the lithosphere, due to its tidal oscillation.

Furthermore, the oscillating lithosphere is charged with energy, due to its deformation as follows:

$$W = \frac{1}{2} (\sigma_1 \epsilon_1 + \sigma_2 \epsilon_2 + \sigma_3 \epsilon_3) \quad (4.1.2.5)$$

Where (**W**) is the potential energy per unit volume, or strain energy per unit volume, (σ_1 , σ_2 , σ_3), are the principal stresses and (ϵ_1 , ϵ_2 , ϵ_3) are the principal strains.

In conclusion, a seismogenic area is charged with a slow, in time, linearly increasing strain, due to the motion of the lithospheric plates and simultaneously, its strain charge oscillates due to tidal forces.

In section (2.5.2), it was pointed out that, an earthquake would occur when the, combined, linearly increasing and oscillating stress reaches the fracture level of the seismogenic area. Moreover, in section (4.1.2), was presented the importance of the normal to the lithosphere force, which triggers its oscillation, and concerns, its effect on the lithospheric, stress-strain charge. Consequently, it is of great interest to know, in advance, the way **the vertical component of the Earth tide evolves in time**, since this is the driving mechanism of the lithospheric, tidal oscillation. The tidal peak values, generated, from the combination of the various Earth tidal components, are the most probable times of occurrence of strong earthquakes (fig. 2.5.2.9).

4.1.3 Generation of Earth Tide Values.

Many scientists have presented Earth-tides generation procedures, in the scientific literature. Some of them are: Doodson (1928), presented an analysis of tidal observations, Pertsev (1958), presented an harmonic analysis of the Earth-tides, Munk et al. (1966), analyzed the frequency spectrum of Earth-tides, Godin (1972), presented an analysis, too, Schuller (1977), used the hybrid least squares frequency domain convolution method in tidal analysis, Rudman et al. (1977), presented a FORTRAN algorithm for the Earth-tide gravity data generation, De Meyer (1982), used a multi input – single output model for the Earth-tide data, Melchior (1983), presented a monograph on Earth-tides, Tamura (1987), calculated the tide generating potential by harmonic analysis, Tamura et al. (1991), used a Bayesian information criterion for tidal analysis, Wenzel (1994), presented the package ETERNA for tidal data analysis, Venedikov et al. (1997), presented a software package for tidal data processing, Venedikov et al. (2000, 2001), calculated the Earth-tide constituents of degree 3 and 4, by using superconductive gravimeters, Venedikov et al. (2003), presented the VAV package for tidal data processing.

Rudman's et al. (1977) methodology addressed, directly, the problem of tidal effects on the gravity measurements in any gravity project. In principle, this methodology corrects the gravity measurement taken, at any place, for the elevation difference which is caused by the tidal waves. This gravity correction is directly, correlated, to the stress-strain oscillating mode of the lithosphere, due to its tidal oscillation. Therefore, graphs of the oscillating gravity corrections (in mgal), generated, for a specific place, indicate, indirectly, its strain-stress oscillating, lithospheric mode. In mathematical terms, it is expressed as:

$$\mathbf{S} = \mathbf{K} \mathbf{T}_c \quad (4.1.3.1)$$

Where: **S** is the oscillating stress-strain component of the seismogenic area

T_c is the tidal gravity correction, calculated, by Rudman's method

K is a constant, which transforms **T_c** into **S**

The methodology, used, by Rudman et al. (1977), is based on the equations which derived by Garland (1965) and Bartels (1957). Vertical derivatives of these potential functions yield the desired components of gravity, in terms of Legendre Polynomials. The implementation of the computer package was based on the work of Goguel (1954) and Longman (1959). Geophysicists used, extensively, this methodology and also, the published, by the European Association of Exploration Geophysicists (EAEG) tables, to apply tidal corrections in gravity surveys, which are dated back for many years.

Samples of tidal gravity correction values have been calculated with Rudma's method for a time period of (2) days, with sampling period of one (1) minute and are presented in the following figure (4.1.3.1).

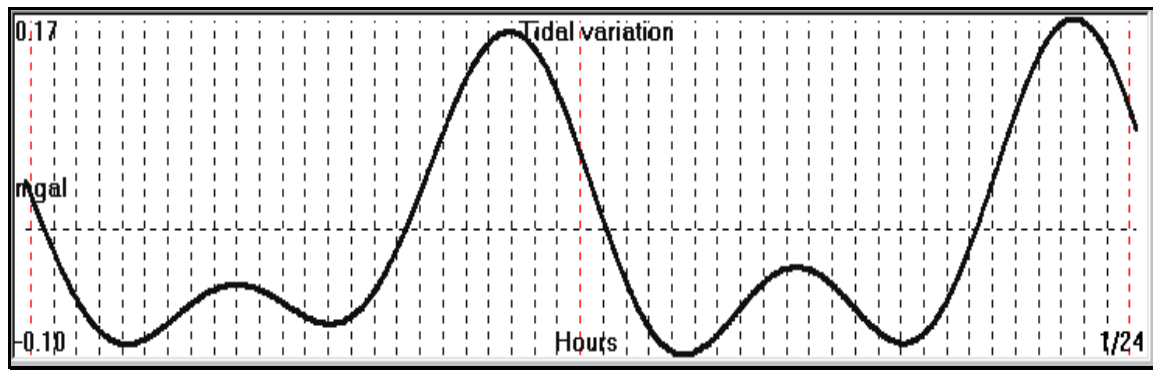


Fig. 4.1.3.1. Gravity correction tidal data was generated by the Rudman's et al. (1977) method, for the period 14-15 February 2007. The dashed, vertical lines indicate hour time period, the red, dashed lines indicate start of the day, and the solid, black line represents the tidal data in mgals.

The 24-hour period oscillation of the Earth's tide is clearly presented, as the 12 hours period is, as well.

If we consider a much longer time period of tidal data, it is possible to filter out periods of a day or less and to visualize oscillations of much more longer periods. This task is performed, simply, by applying Shannon's sampling theorem. If a data series is sampled by a sampling interval of Δt , then the lowest period which is preserved in the sampled data set, is $2\Delta t$ (Nyquist period). The entire operation behaves as a low-pass filter.

In the previous case (of longer data set), we apply a sampling interval of one (1) day. Therefore, daily tidal oscillations will be filtered out, since the maximum period, preserved, in the sampled data, is two (2) days. The result of such an operation is demonstrated in the following figures (4.1.3.2 – 4.1.3.3).

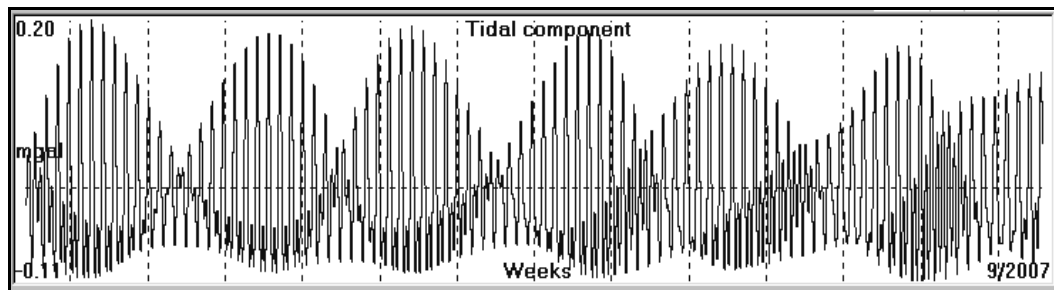


Fig. 4.1.3.2 A three-months period (December 2006 – February 2007) of tidal data set, sampled at one-minute interval, is presented.

The result of the application of the re-sampling operation, at a day's sample period, on the tidal data of figure (4.1.3.2) is the data set presented, in the next figure (4.1.3.3).

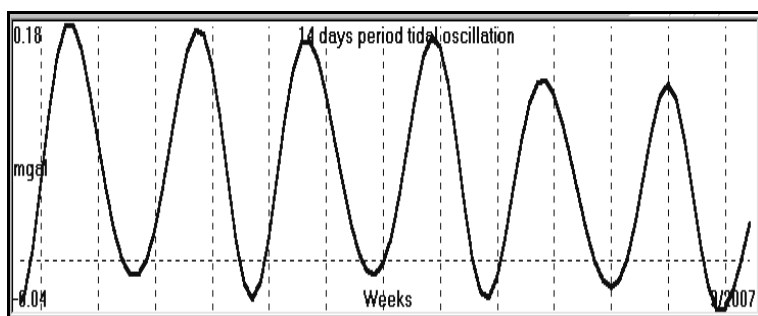


Fig. 4.1.3.3. A three-month period (December 2006 – February 2007) of tidal data set, re-sampled at one-day interval, is presented. The tidal oscillation resembles the M1, Moon declination component.

Next, it is considered a much longer period of four (4) years, with a day's sampling interval (**fig. 4.1.3.4**). In this case, are observed two distinct tidal oscillations. The first one which is of the longest period corresponds to the yearly component of the tidal gravity variations. On top of it is the 14 days period oscillation of the previous figure (**4.1.3.3**).

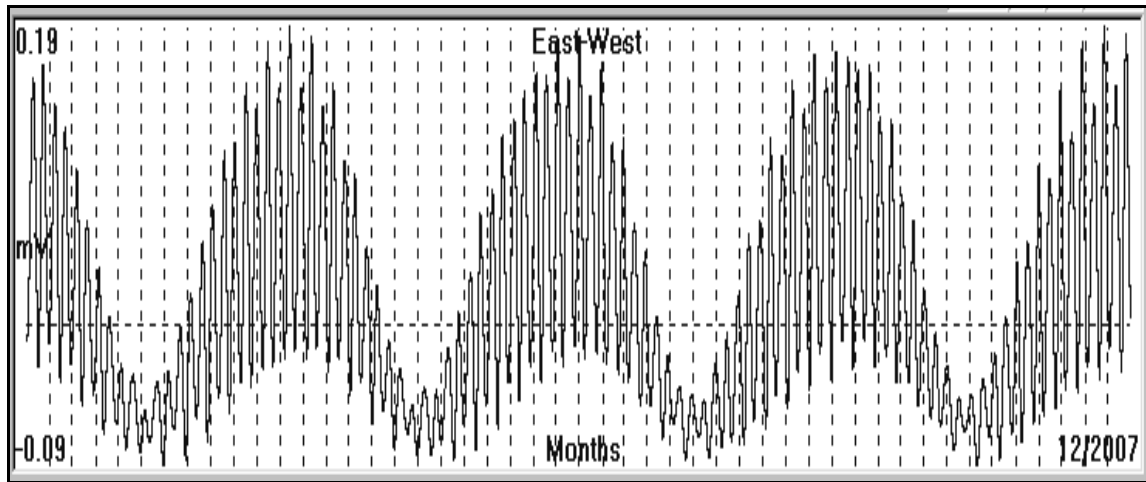


Fig. 4.1.3.4. Four years period (2004 – 2007) of tidal gravity data (sampled at one day) are presented. The yearly component is superimposed by the 14 days period tidal oscillation.

The graphs of figures (**4.1.3.2 - 4.1.3.4**) have been calculated for the following geographical parameters:

Latitude : $38^{\circ}, 0', 0''$ (Athens location)
Longitude : $26^{\circ}, 0', 0''$ „
Height : 0m a.s.l
Time zone : 0

So far, specific peaks of tidal oscillation have been identified. Starting from yearly period, these peaks span down to 12-hour periods. Following the analysis which was presented earlier in section (**4.1.2**), these peaks correspond to stress-strain peaks of the seismogenic area, which is affected by the tidal waves. Therefore, the seismicity which is induced, by the lithospheric oscillation, must coincide with the corresponding, tidal peaks. This will be investigated as follows:

4.1.4. Seismicity compared to one year's period Earth-tide wave.

The longest period which has been identified so far in the tidal data, is a year's period. Following the previous analysis, this type of lithospheric oscillation strain-stress charge must be mirrored into the seismicity of a seismogenic region for the same period of time. To this purpose, the seismic events, per 10 days period of time, are correlated to the corresponding lithospheric plate oscillation for a period of a year (2000). The entire Greek territory is considered as a seismogenic area. This is presented in the following figure (**4.1.4.1**). The yearly period Earth tide wave is presented in the upper graph, while the “per 10 days seismic events”, are shown in the lower graph.

It is evident that the seismicity increases and correlates well with the increase of the amplitude of the yearly, tidal wave.

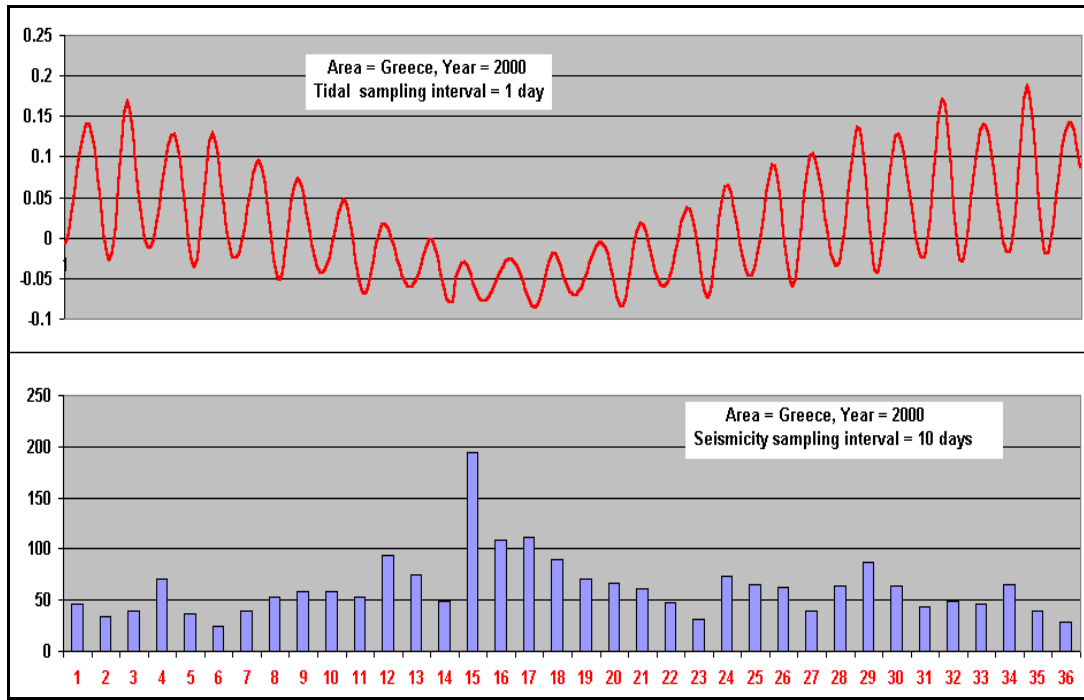


Fig. 4.1.4.1. Yearly Earth-tide wave compared with the seismicity for the same period of time.

These results strongly suggest the dependence of seismicity of a seismogenic area to Earth-tide waves, as a triggering mechanism, as has already been pointed out by earlier papers. In terms of time prediction it suggests that **the predictive time window can be of the order of a few months**, by assuming that a strong earthquake will occur within this year's period of time.

4.1.5. Seismicity compared to 14 days period lithospheric oscillation.

If we consider shorter wavelengths of the lithospheric plate tidal oscillation, then more interesting results are found. In next figure (4.1.5.1), is demonstrated the dependence of seismicity to the $T=14$ days oscillation of the Earth-tide for the period 17/04/2001 – 11/05/2001. At the same period of the time only one ($M_s = 5.4R$, 01/05/2001) strong earthquake occurred. This seismic event occurred very close to the negative peak of the tidal oscillation amplitude, following the already, presented, theoretical analysis.

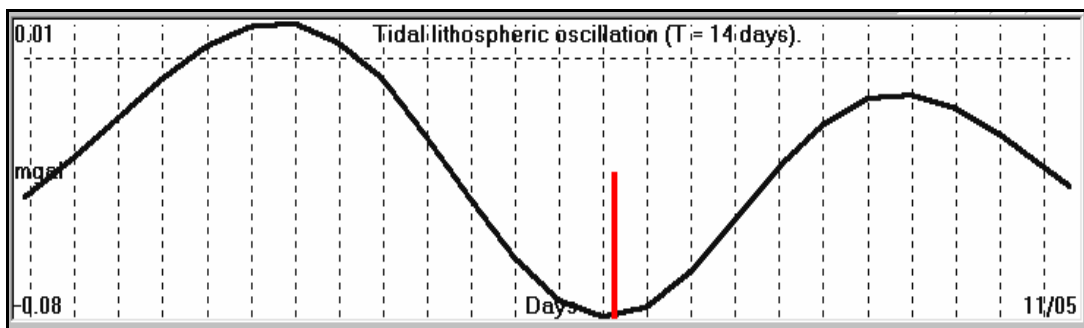


Fig. 4.1.5.1. Seismicity compared to 14-day Earth-tide oscillation for the time period 17/4 – 11/5/2001. The red bar indicates the occurrence of the earthquake ($M = 5.4R$).

The strongest and only one seismic event, EQ (5.4R), occurred on top of the minimum peak of the tidal wave in this period of time.

4.1.6. Daily Earth-tide oscillation, correlated, to same day seismicity (29/05/2001).

The same mechanism holds for the day when a strong EQ occurs. The final extra stress load which is necessary to trigger a strong EQ is provided by the day's oscillation of the Earth-tide. Therefore, the EQ will, most probably, occur at one of the four tidal peaks which exist in a day's tidal oscillation (Thanassoulas et al. 2001). The EQ of the figure (4.1.5.1) is compared with the Earth-tide variation of the day of its occurrence (fig. 4.1.6.1).

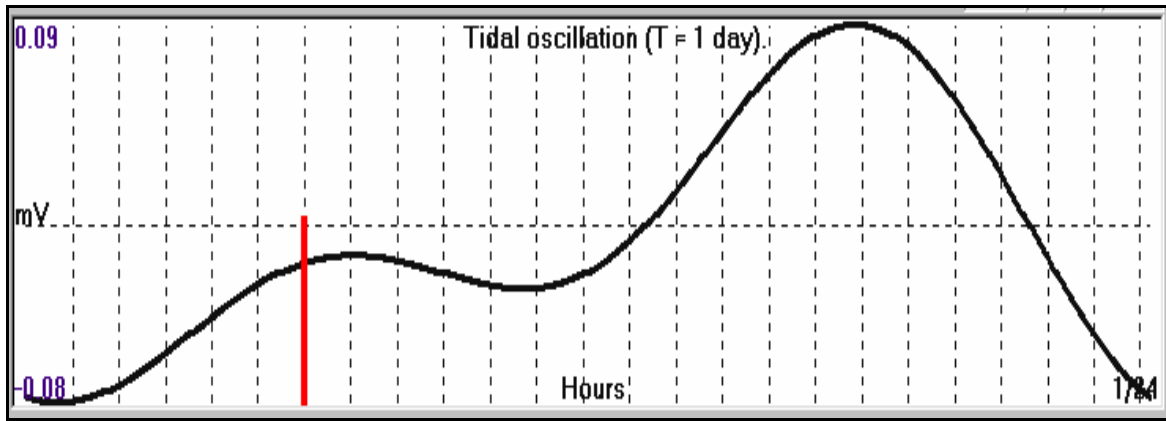


Fig. 4.1.6.1. EQ occurrence time compared with the Earth-tide variation of the day of its occurrence.

The same EQ, in figure (4.1.6.1), coincides very well with the first maximum of the Earth's daily tidal wave (12hour period oscillation) in its day of occurrence span.

4.1.7. Examples of “a posteriori” correlation of Earth-tide waves to seismicity.

Since the tidal waves excite the lithosphere in an oscillatory mode, the triggered, seismicity must correlate to the most basic frequencies of tidal waves. This is demonstrated as follows.

The seismicity for the period 1995 – 2001 and for seismic events stronger than 5.5R for the Aegean area is compared with the yearly period tidal waves (fig. 4.1.7.1).

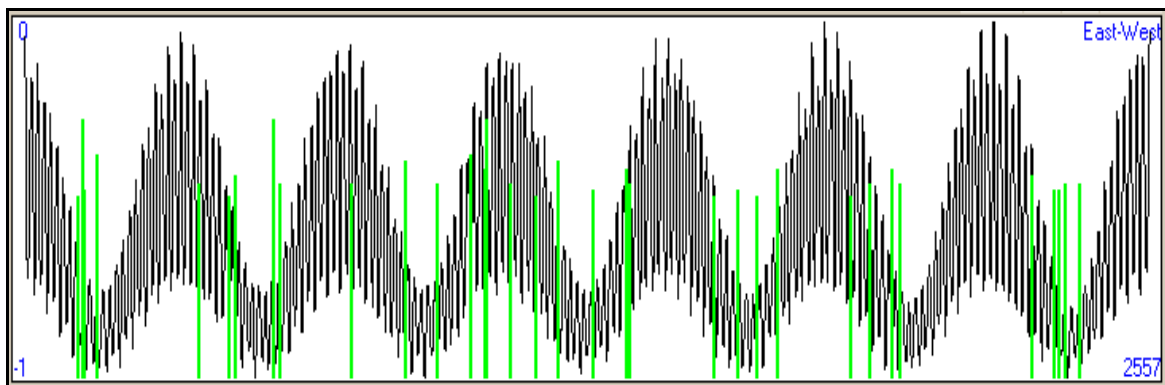


Fig. 4.1.7.1. Yearly tidal oscillation, for the period 1995 – 2001, compared to seismicity (green bars) of the same period.

The seismic events, as a general observation, are clustered at the “lows” of the oscillation (mainly during June-July), while some exceptional seismicity exists during years 1997-1998.

The same correlation, between tidal waves and seismicity, holds for the 14 days period oscillation. This is demonstrated in figure (4.1.7.2).

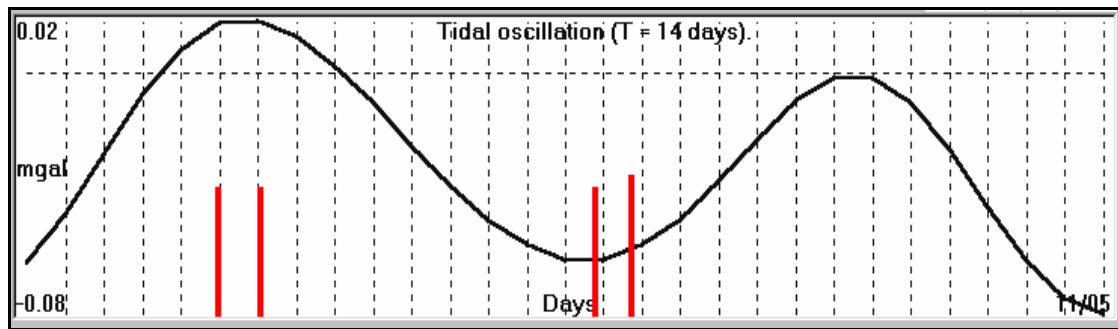


Fig. 4.1.7.2. 14 days period oscillation, for the period 13/04/2000 – 10/05/2000, compared with the seismicity (red bars, $M_s > 5.0R$) of the same period.

The two double, corresponding seismic events occurred during the low and high peak of the tidal oscillation.

Finally, the correlation of the time when a strong EQ occurred, to the daily tidal oscillation, is presented (Thanassoulas et al. 2001), in the following fig. (4.1.7.3).

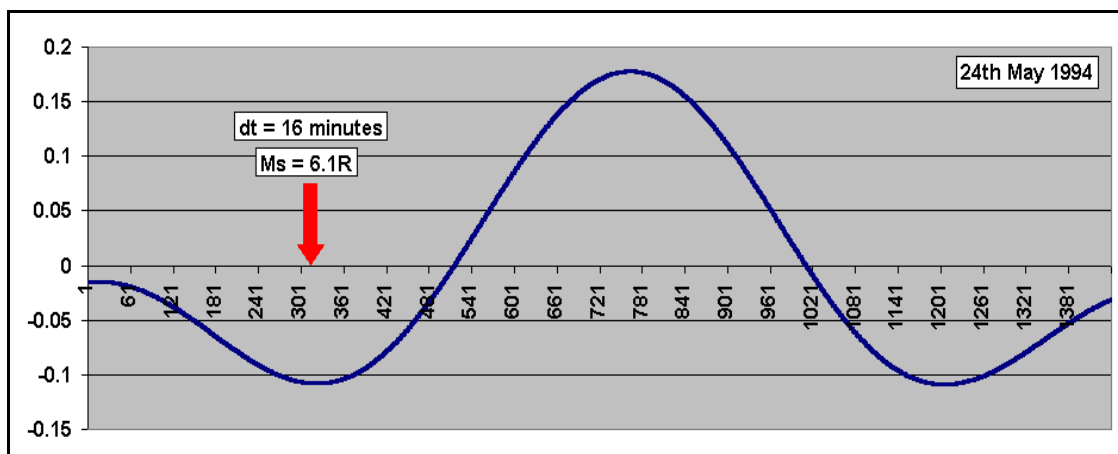


Fig. 4.1.7.3. Daily, tidal variation, compared to the time when a strong EQ occurred. The red arrow indicates the EQ time of occurrence. The time difference between the tidal peak and the time of occurrence is only 16 minutes.

It is evident, that strong EQs, do not occur at random times, but they follow, quite well, the amplitude peaks of the tidal wave oscillation, and follow the triggering mechanism, presented in figure (2.5.2.9)

4.1.8. Statistical test of seismicity to 14days period tidal oscillation.

In order to verify the validity of the tidal oscillations to the seismicity of a seismogenic area, a study has been performed on strong EQs ($M_s > 5.5$) for the period 1995 – 2001, which are initially, compared, to the 14 days period tidal wave. The total number of the seismic events which are studied is forty (40).

The “by chance” percentage (P_{ch}) of the estimation of the correct day of the occurrence of a strong EQ is:

$P_{ch} = 14.28\%$ for a half period (7 days).

In the following table (1) are presented the EQs which were used in this study. The first column indicates the time in the format **yyyymmddhhmm**, the next two are the geographical coordinates, while the next two are the depth of an EQ in Km and its magnitude in **M_L** , (**$M_s = M_L + 0.5$**).

TABLE – 1

199505040034	40.57	23.69	7	5.0	199803091121	36.04	28.49	54	5.0
199505130847	40.18	21.71	39	6.1	199804290330	35.99	21.98	5	5.5
199505150413	40.06	21.68	5	5.0	199807161729	38.66	20.56	5	5.1
199505170414	40.07	21.69	5	5.1	199809302342	41.93	20.57	32	5.4
199506150015	38.37	22.15	26	5.6	199810061227	37.19	21.13	5	5.2
199506150030	38.33	21.93	5	5.2	199810080350	37.79	20.27	5	5.2
199602011757	37.72	19.85	1	5.2	199904170817	35.97	21.65	32	5.0
199604121539	36.62	27.09	156	5.0	199906110750	37.56	21.11	58	5.1
199604260701	36.42	27.99	63	5.3	199907250656	39.30	27.79	28	5.0
199607200000	36.11	27.52	38	6.1	199909071156	38.15	23.62	30	5.4
199608052246	40.07	20.67	1	5.2	200002221155	34.75	25.53	36	5.0
199701121210	40.97	19.29	5	5.2	200004050436	34.22	25.69	38	5.2
199705160700	41.02	20.33	5	5.5	200005240540	36.00	22.01	5	5.4
199707271007	35.28	21.00	40	5.2	200005260128	38.91	20.58	5	5.3
199710131339	36.41	22.18	6	5.6	200006130143	35.12	27.19	37	5.2
199711142138	38.80	25.87	25	5.4	200104091738	40.05	20.44	27	5.3
199711181307	37.26	20.49	5	6.1	200105290444	35.63	27.81	5	5.1
199711181313	37.36	20.65	5	5.6	200106101311	38.47	25.59	32	5.1
199711181523	37.25	21.16	16	5.0	200106230652	35.65	28.40	56	5.2
199801101921	37.12	20.73	5	5.2	200107260021	39.05	24.35	19	5.2

The statistical analysis of the data of table (1), compared, with the corresponding 14 days period tidal oscillation, gave the following results:

Mean value of time difference of the time of occurrence of the EQs, from the corresponding tidal peak values, for the entire data set, equals to **1.18 days**.

dt Mean Value = 1.18 days
S. Dev. Of dt = 1.15 days

Percentage of EQs with dt = 0 days equals to 39.47% (exact day)
Percentage of EQs with dt = 0 - 1 days equals to 50.00%
Percentage of EQs with dt = 0 - 2 days equals to 78.95%
Percentage of EQs with dt = 0 - 3 days equals to 100.00 %

A direct comparison of the “by chance” P_{ch} value (14.28%) to the percentage (**39.47%**) of EQs, which coincide in time (day) to the tidal peak oscillation, suggests that strong EQs ($M \geq 5.5$) can be assigned a time predictive window, as narrow as close to a day's time period. If wider predictive time windows are assumed, then this comparison becomes even better, reaching a value of 100%, for a time window of three (3) days.

4.1.9. Statistical test of seismicity to daily tidal oscillation.

Furthermore, is studied the correlation of the time of occurrence of strong earthquakes to the exact time of peak values of the daily Earth-tides. The data which were used were obtained from the Geodynamic Institute of Athens, for the time period from 1964 to 2001.

EQs with $M_s \geq 6R$ were selected totaling to a number of (70).

For each one of the selected EQs the Earth-tidal was calculated for its day of occurrence and was determined the difference in minutes (**dt**) between the time of occurrence and the appropriate Earth-tide peak value.

The basic assumption that the triggering of the earthquakes (Knopoff 1964, Shlien 1972, Heaton 1982, Shirley 1988), is mainly due to lunar or lunisolar components (**K2, S2, M2**) that exhibit a periodicity of almost 12 hrs, was adopted before any further processing of these data commences. By using the **M2**, as a basic periodicity, the **T/2** time, between two successive Earth-tide peaks, equals to **372.6** minutes.

Starting from this assumption, the calculated probability, for a “by chance” coincidence of the time of occurrence of a strong EQ, with the time of the peak value of the Earth-tide for the same day, using different time-windows, is as follows:

Window of:

1hr:	$P_{1hr} = 60/372.6 = 0.161$ or 16.1%
2hr:	$P_{2hr} = 120/372.6 = 0.322$ or 32.2%
3hr:	$P_{3hr} = 180/372.6 = 0.483$ or 48.3%

The calculated **P** values indicate the threshold, to be considered, between **the random correlation** of the Earth-tide peak values and the time of occurrence of each EQ of the data set, on one hand, and the **well behaved one** on the other, in other words “**above what level, a P value is worth to be considered**”.

For the statistical test of the theoretical model, postulated, the following calculations were made:

Overall mean dt, calculated, for all EQ of the data set.

$$MV = 92.66 \text{ minutes } (\Sigma dt/70)_{70}$$

The mean value of the discrepancy between the time of occurrence of the Eqs used and the corresponding Earth-tide peak values is: **1h 34 min.**

Window of : 1 hour

No. of EQs	: 26	
P value	: 0.371	37.1%
Mean Value (MV)	: 32.46 minutes	

Window of : 2 hours

No. of EQs	: 44	
P value	: 0.629	62.9%
Mean Value (MV)	: 53.90 minutes	

Since the calculated value of **P**, for both windows used, is larger than the corresponding **P** value for the “by chance” cases, it suggests that, by using both time-windows, the theoretical model follows **a driving mechanism which is not random.**

The same processing was applied on the data set for **different windows of M_s values.** The results are as follows:

Magnitude window (M_s) = 6.0 – 6.5 R.

Total No. of EQs	: 55
-------------------------	-------------

Time window	: 1 hr
No. of EQs within time window	: 17
P value	: 0.309 - 30.9%

Time window	: 2 hours
No. of EQs within time window	: 32
P value	: 0.582 - 58.2%

Magnitude window (Ms) = 6.5 – 7.0 R.

Total No. of EQs	: 14
Time window	: 1 hr
No. of EQs within time window	: 9
P value	: 0.643 - 64.3%

Time window	: 2 hours
No. of EQs within time window	: 11
P value	: 0.786 - 78.6%

Magnitude window (Ms) = 6.5 – 7.5 R.

Total No. of EQs	: 6
Time window	: 1 hr
No. of EQs within time window	: 3
P value	: 0.500 - 50.0%

Time window	: 2 hours
No. of EQs within time window	: 5
P value	: 0.833 - 83.3%

In the last case, there was an overlap on the data set, in order to overcome the limited number of EQs available, with an Ms value larger than 7.0R.

The following figures have been prepared for a better demonstration of the “**coupling mechanism**” which exists between the time of occurrence of a strong earthquake and the corresponding Earth-tide peak value. The time scale corresponds to local time. The red arrows indicate the time of earthquake occurrence in local time. The blue line of the graph is the Earth-tide oscillation in local time, too.

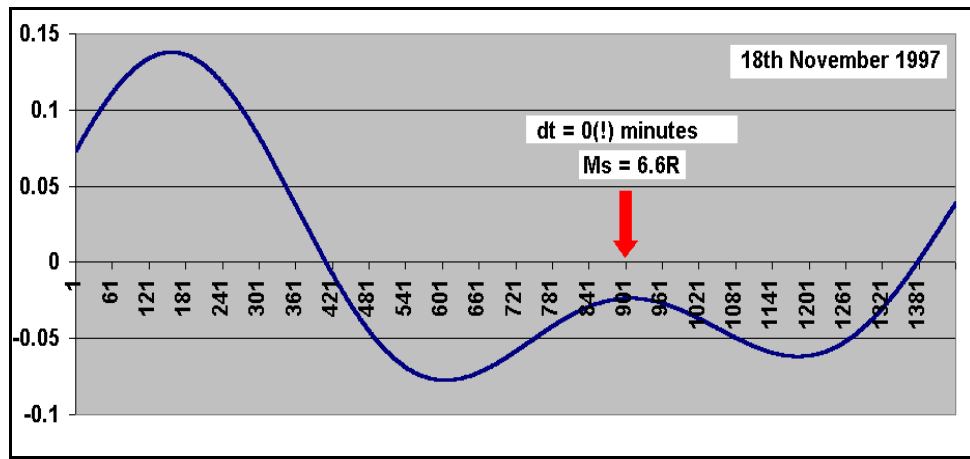


Fig. 4.1.9.1. Correlation of the EQ on 18th November 1997 time of occurrence, with the corresponding Earth-tide peak.

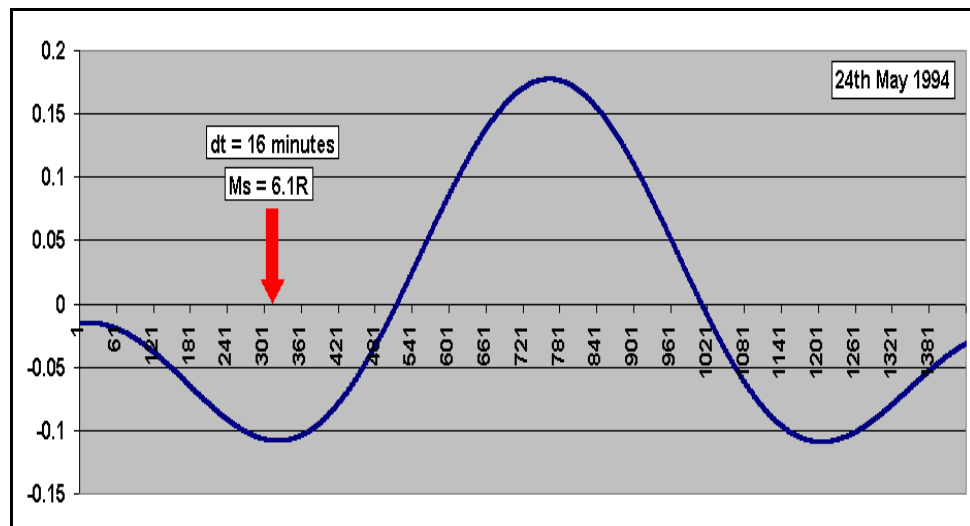


Fig. 4.1.9.2. Correlation of the EQ on 24th May 1994 time of occurrence, with the corresponding Earth-tide peak.

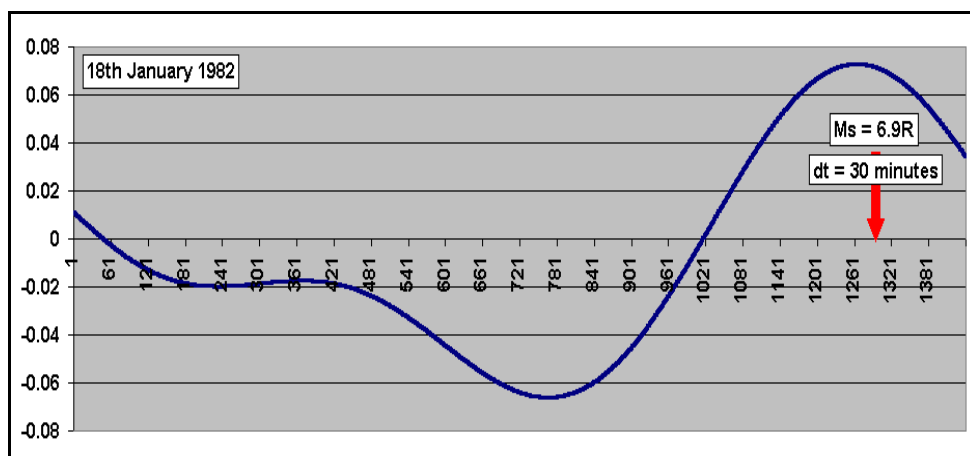


Fig. 4.1.9.3. Correlation of the EQ on 18th January 1982 time of occurrence, with the corresponding Earth-tide peak.

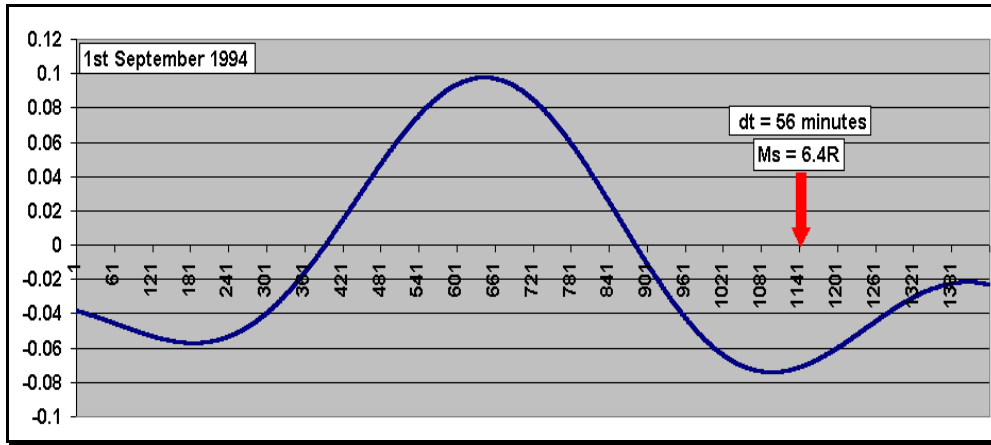


Fig. 4.1.9.4. Correlation of the EQ on 1st September 1994 time of occurrence, with the corresponding Earth-tide peak.

The same methodology was applied on EQs ($M_s \geq 4.0R$), which occurred between the 1st and 22nd February 2001. Although the statistical sample is small, it is indicative for the validity of the methodology.

Magnitude window $M_s \geq 4.0 R$ (February 2001)

Total No. of EQs	: 7
Time window	: 1 hr
No. of EQs within time window	: 2
P value	: 0.286 28.6%
Time window	: 2 hours
No. of EQs within time window	: 5
P value	: 0.714 71.4%

The following figures demonstrate the methodology, which is applied on EQs of February, 2001 with a magnitude $M_s \geq 4.0R$, except the first one, which corresponds to the EQ that occurred in Athens.

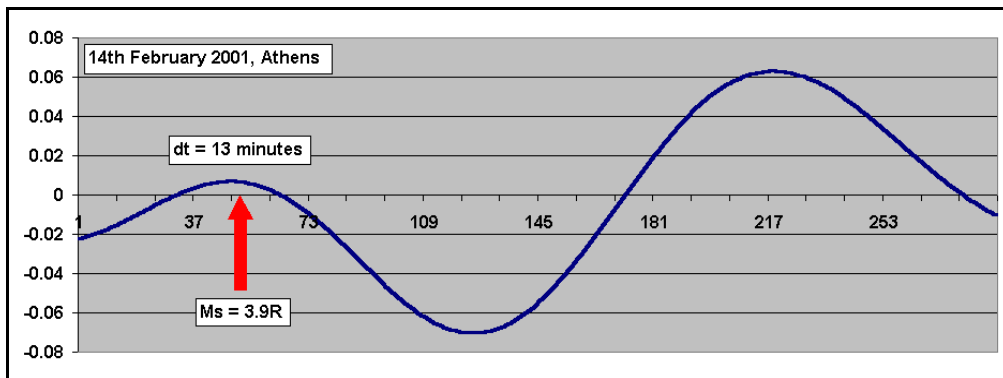


Fig. 4.1.9.5. Correlation of the EQ on 14th February 2001 time of occurrence, with the corresponding Earth-tide peak.

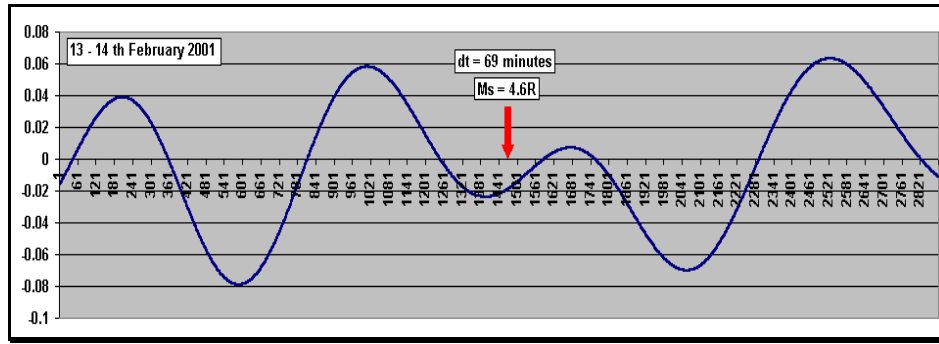


Fig. 4.1.9.6. Correlation of the EQ on 14th February 2001 time of occurrence, with the corresponding Earth-tide peak.

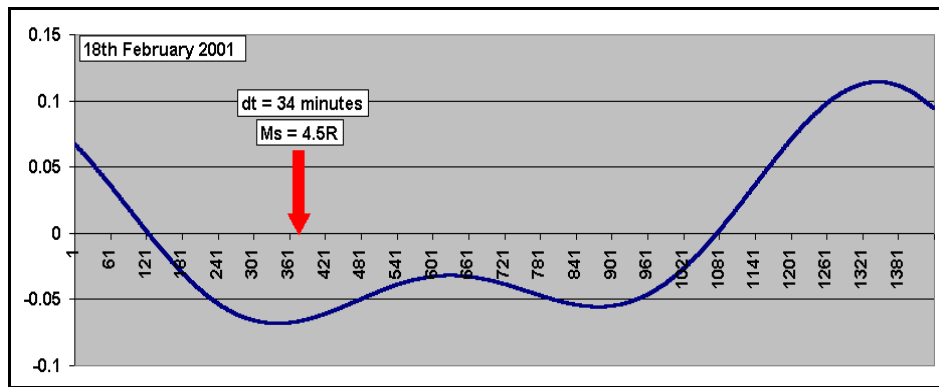


Fig. 4.1.9.7. Correlation of the EQ on 18th February 2001 time of occurrence, with the corresponding Earth-tide peak.

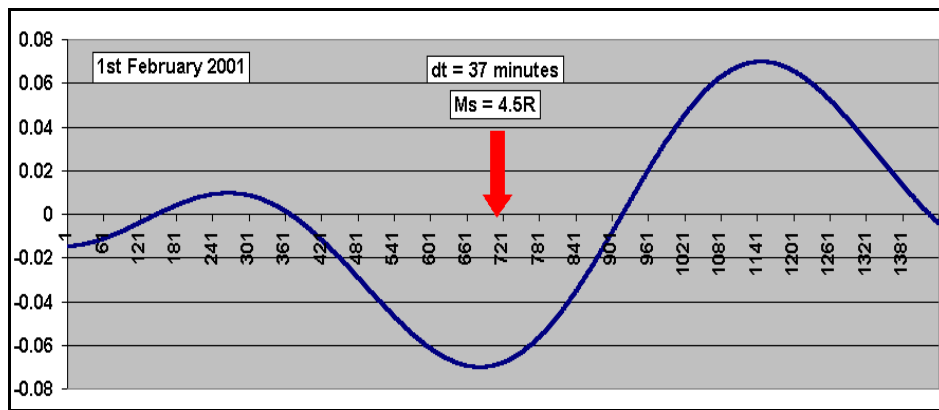


Fig. 4.1.9.8. Correlation of the EQ on 1st Feb. 2001 time of occurrence, with the corresponding Earth-tide peak.

When the strong correlation which is observed, between the time of occurrence of strong EQs and the 14 days period tidal wave, is combined with the daily, tidal variation, it facilitates the estimation of a very narrow, predictive time-window for the imminent, strong EQ, with very large probability.

What has been demonstrated from the previous, presented, cases is the following:

- Earthquakes, in their vast majority, occur when the stress-strain of the seismogenic region acquires its peak stress-strain level.

- The time of occurrence of the stress-strain change of a seismogenic area, is strongly correlated, to the tidal peak values of the lithospheric oscillation.
- The time of occurrence of the tidal peaks is well known in advance, from the analysis of the tidal gravity waves, related, to any seismogenic area.
- Within a year's period, strong earthquakes (if any) will mostly take place in specific times, predefined, by the analysis of the tidal, lithospheric oscillations.

In practice, it is postulated that, with an assumed, predictive time window of +/- 2 days, **there are only 52 specific times within a year's period (the weekly tidal oscillation peaks) when a strong earthquake can occur.**

Assuming a more narrow predictive time window (of +/- 2 hours), then the number of times when a strong EQ can occur within a year increases to:

$$\text{Times} = \text{weeks} \times 4(+/-2\text{days/peak}) \times 4(\text{daily tidal peaks})$$

$$\text{Times of occurrence} = 52 \times 4 \times 4 = 832.$$

The calculated number of times of occurrence, of a strong EQ, within a year's period, although it looks large, it is definitely a "small number", compared, to the infinite times of occurrence, suggested, from equation (4.1.1.5) and the various, proposed, models, in figures (4.1.1.1), (4.1.1.2), (4.1.1.3).

The procedure which has already been demonstrated, by the study of the maxima – minima of the tidal, lithospheric oscillation, can be represented with a Boolean "AND" operation. The infinite space of time of occurrence solutions, suggested, by the equation (4.1.1.5) are subjected to an "AND" operation with the space of "tidal oscillations". This appears in the following figure (4.1.9.9)

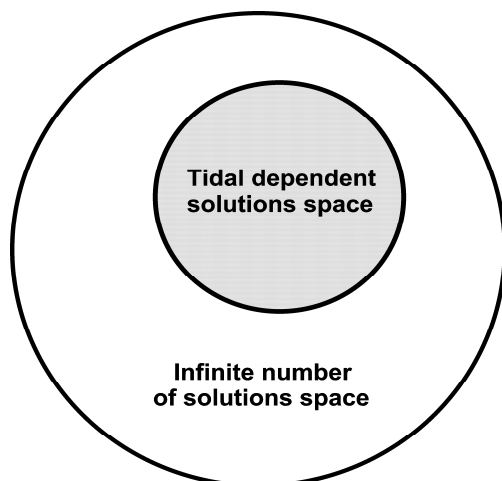


Fig. 4.1.9.9. The infinite space of time of occurrence solutions (outer circle), suggested, by the equation (4.1.1.5), is subjected to an "AND" operation with the space (inner, shaded circle) of "tidal oscillations" times of maximum amplitude.

Although, there is an improvement in the calculation of the predictive time window of the occurrence of a strong EQ, this is not enough for short-term prediction. Actually, it is not practical, at all, in predictive terms. If there is no way to identify at which "tidal peak", within a year's period, an EQ will occur, then the entire scheme is no longer a "short-term" prediction, but it becomes rather a "medium-term" one. This type of prediction can be treated by the already, referred, statistical methods.

Therefore, there is the necessity to constrain further more the "predictive time window" solutions, obtained, so far. Actually, the target is to distinguish the "candidate" tidal peaks when a strong EQ will occur. This may be achieved by further constraining, the already, determined, (832) time solutions, by the properties of the "electrical signals generating mechanisms", which already have been presented in section (3).

4.1.10. Electrical signals timing, compared, to lithospheric tidal oscillations.

The electric, seismic precursory signals which are presented to date in the seismological literature are distinguished in the following main types:

- a) **SES**, (Seismic Electric Signals) or “high frequency” signals.
- b) **Oscillating signals**, mainly of 24 hours / 14 days period following the tidal oscillation.
- c) **VLP** signals, (Very Long Period).

Examples of such signals have already been presented in section (3). A thorough study of the various mechanisms which generate electrical signals, suggests that the piezoelectric is the most probable one. This is the only mechanism that justifies in total: the generation of **SES** (signals, due to higher order derivatives of the non-linear part of the generated potential), **Oscillating signals**, (due to the oscillating component of the stress-strain of the seismogenic area, caused, by the oscillatory effect of the Earth-tides upon the stress-strain / piezoelectric potential curve) and the **VLP** signals, (due to the total form of the generated static potential which is caused by the large scale crystal-lattice deformation).

The correlation of such signals with the tidal oscillations will be demonstrated through specific examples, since strong EQs are not a routine event, thus prohibiting us to apply statistical validation by using a large number of statistical samples.

a. **SES, (Seismic, Electric Signals) or “high frequency” signals.**

SES generated by the Izmit, (17/8/1999, M=7.5) EQ, in Turkey.

The electrical signals, which were recorded in Volos (**VOL**), Greece (Thanassoulas et al. 2000) before the Izmit, EQ (17th, August, 1999, M=7.5) in Turkey, will be the first example to be demonstrated. The detailed study of the recordings of the Earth's electrical field by (**VOL**) monitoring site, for a period of almost three months before the Izmit EQ, revealed the existence of high frequency (**SES**) electrical signals. These signals were observed almost right from the start (21st June, 1999) of the recording period and consequently it is justified to accept their earlier start-up time of origin.

Samples of these signals are presented bellow. During a six months period of recording of the Earth's electric field, only the **NS** component was recorded by **VOL** monitoring site. The following figure (4.1.10.1) corresponds to the recording day on 21/06/99. This recording was performed almost two months before the strong Izmit, (16/8/1999, M=7.5) earthquake in Turkey.

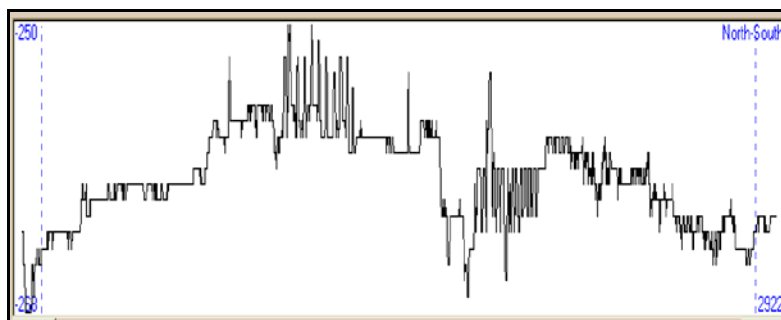


Fig. 4.1.10.1. Electrical signals, recorded on 21 / 06 / 1999 by **VOL** monitoring site, at **NS** direction.

Next data set corresponds to the recording day on 22/07/99. That is almost after a month later than the previous one and almost one month before the Izmit EQ.

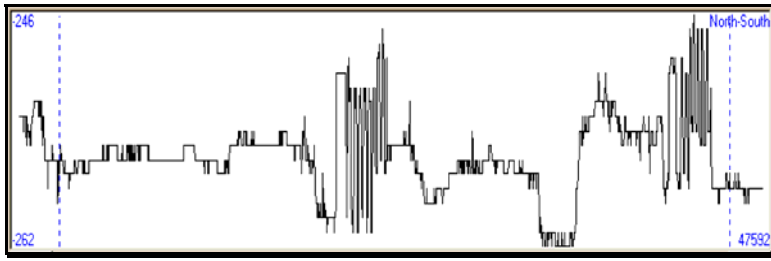


Fig. 4.1.10.2. Electrical signals recorded, on 22 / 07 / 1999 by **VOL** monitoring site.

Similar electrical signals have been observed in this recording, too. Almost in the entire time of recording, are observed two distinct signals, separated, at a certain period of time, of some hours. Next one was recorded on 03/08/99.

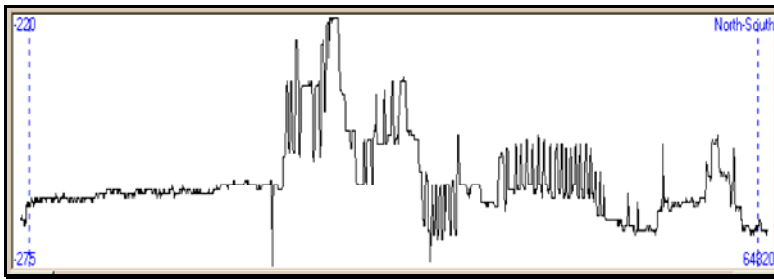


Fig. 4.1.10.3. Electrical signals recorded, on 03 / 08 / 1999 by **VOL** monitoring site.

The next one is a two days recording from 13 to 14/08/99. That is a very short time, before Izmit EQ (17-08-1999) occurred.

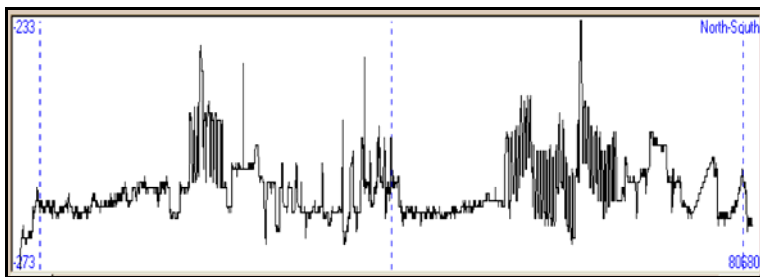


Fig. 4.1.10.4. Electrical signals recorded, on 13 – 14 / 08 / 1999 by **VOL** monitoring site.

The last one (**fig. 4.1.10.5**) had been recorded between 17-18/12/99. By that time, the most of the stress load of the seismogenic area had been released and, consequently, the SES signals disappeared. This is demonstrated, clearly, by the following figure (**4.1.10.5**).

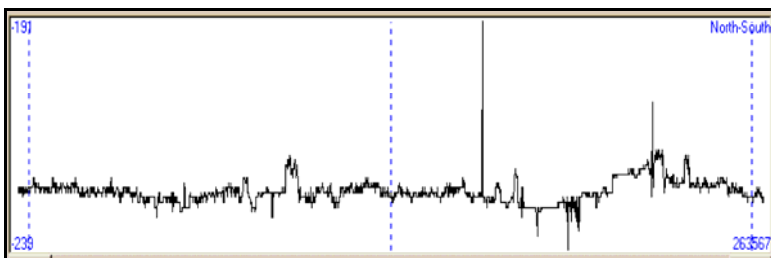


Fig. 4.1.10.5. Electrical field recorded, between 17-18 / 12 / 1999, by **VOL** monitoring site.

The absence of electrical signals, comparing to previous figures, is characteristic.

Another interesting observation is that, the start time of these signals coincides with two specific daytimes.

The first one is around 9a.m, while the second one is around 21.5 p.m. This observation was studied, in detail, by separating the “9.0a.m” signals and the “21.5 p.m” signals in two groups (signal – **A**, signal - **B**).

The following figure (4.1.10.6) represents the existence of electrical signals (signal – **A**) as a function of time (in days), while the vertical axis represents the startup time of each signal (in minutes) in the span of the day of its occurrence.

In the horizontal axis of time, the earthquakes in Izmit, Athens and Duzce are marked with a red arrow.

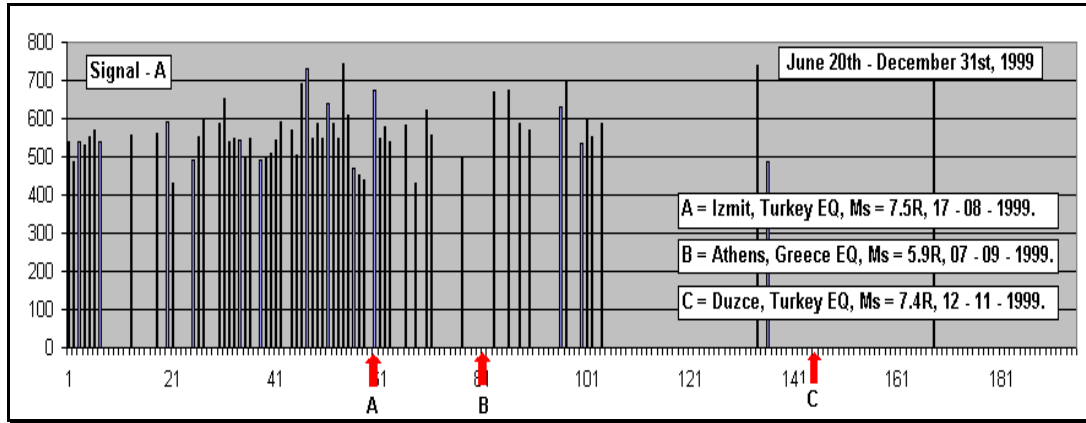


Fig. 4.1.10.6. Daily presence of signals – **A** is shown, between 20/06 – 31/12/1999.

In the following figure (4.1.10.7), the signals - **B** are presented with the same annotation.

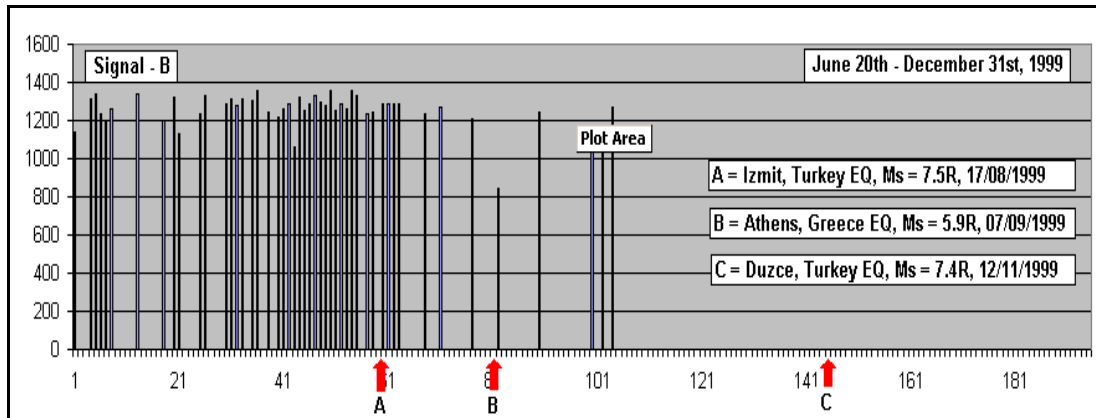


Fig. 4.1.10.7. Daily presence of signals – **B** is shown, for the period 20/06 – 31/12/1999.

What is clear, from both figures, is the drastic decrease of the presence of the signals after the occurrence of Izmit EQ. On the other hand, before Duzce EQ, of a similar magnitude to Izmit EQ, no such signals were observed. This suggests that Izmit – Duzce regions may be considered as a unit area, stress loaded and seismically activated. Consequently, the generated, electrical signals were produced by the entire, seismically active area and not only by Izmit focal region. This is corroborated from the fact that IZMIT – DUZCE distance is of the order of 80Km which coincides quite well with the expected fracture length of the seismogenic fault, which is what is more or less expected for an EQ of $M = 7.5$.

Therefore, when most of the stresses load of the entire area had been released (by Izmit EQ), the rest of it was not capable of generating similar, electrical signals. Viewing this pair of strong EQs from the point of view of electrical signals generation mechanism, it is a very interesting and spectacular, seismic event.

For both signals (**A**, **B**) the mean starting time has been calculated. For signals (**A**) the mean value (MV_A) was calculated as **569** minutes.

$$MV_A = 569 \text{ minutes}$$

(4.1.10.1)

This corresponds to a mean starting time of 9hr 29 minutes. For signals **(B)**, the same calculation results in a **(MV_B)** of **1257** minutes. This corresponds to a mean starting time of 20hr 57 minutes.

$$MV_B = 1257 \text{ minutes}$$

(4.1.10.2)

Finally, the mean time difference in time of occurrence of the electrical signals has been calculated, as:

$$MV_B - MV_A = 11\text{hr } 28 \text{ minutes.}$$

(4.1.10.3)

Comparing this result to the Earth-tide components, its very close resemblance is revealed to **(K₂)** (lunisolar) and **(S₂)** (principal solar) components. A discrepancy of 4.17% has been calculated for the **(K₂)** component, while a value of 4.4% corresponds to the **(S₂)** one. The satisfactory results fit what was expected from the earlier theoretical analysis.

In simple words, the entire Izmit-Duzce seismogenic area was at such critically point of stress-strain charged conditions, so it generated SES twice in a day, at the peaks of the 24 hours lithospheric oscillation.

Below are **(SES)** sample signals, recorded, by **(HIO)**, **(PYR)** and **(ATH)** monitoring sites, and compared to the 14 days period tidal, lithospheric oscillation local peak value.

SES signals recorded at HIO monitoring site, compared to 14 days period tidal lithospheric oscillation.

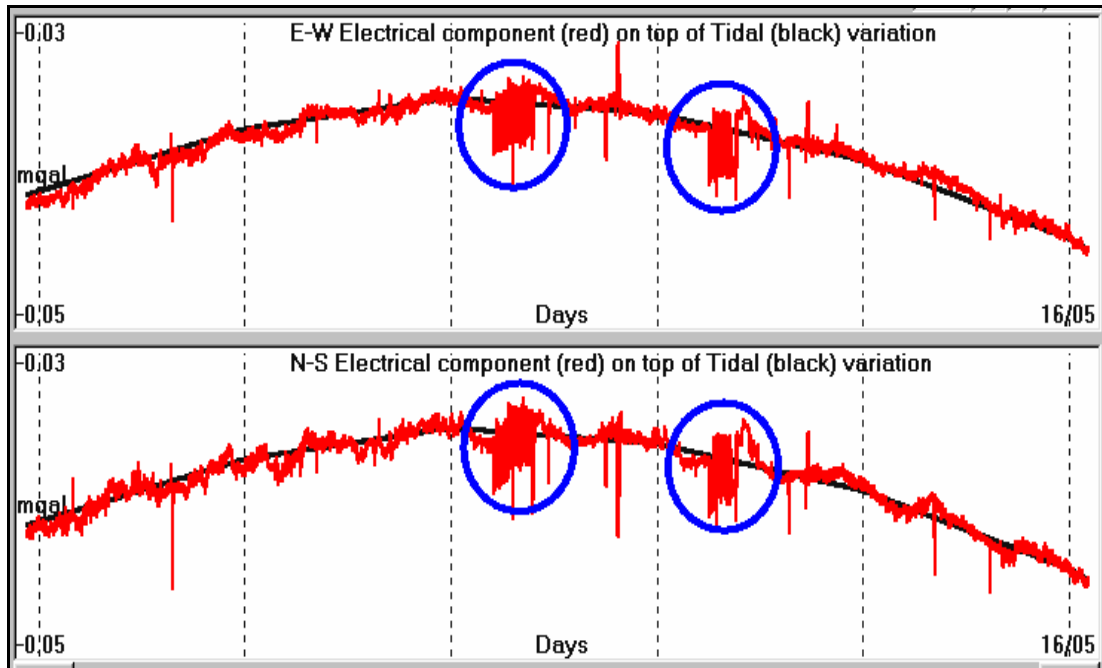


Fig. 4.1.10.8. **SES** precursory, electrical signal (in blue circles) recorded, by **HIO** monitoring site, between 13 and 14 May 2006 (HIO060513-14).

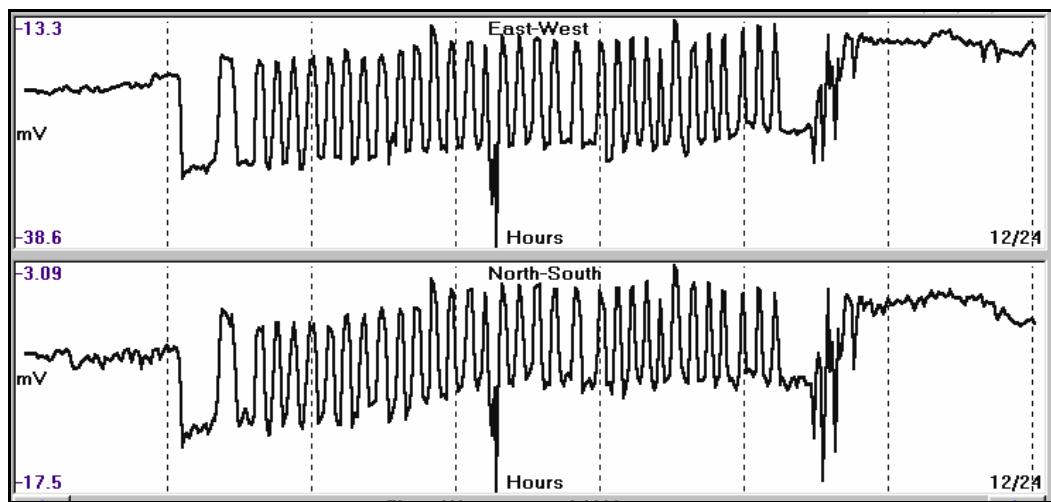


Fig. 4.1.10.8.a. Zoom-in of the left **SES** signal of fig. (4.1.10.8).

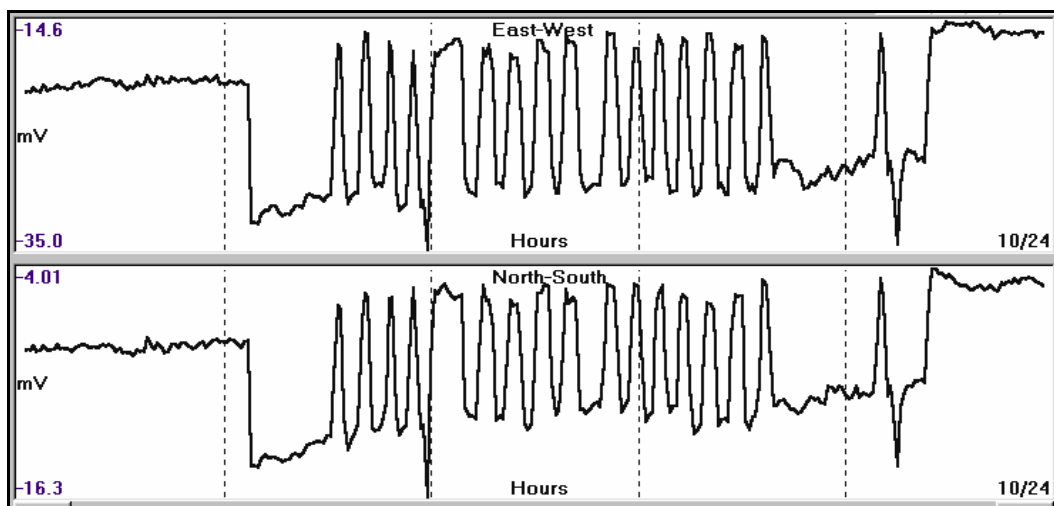


Fig. 4.1.10.8.b. Zoom-in of the right **SES** signal of fig. (4.1.10.8).

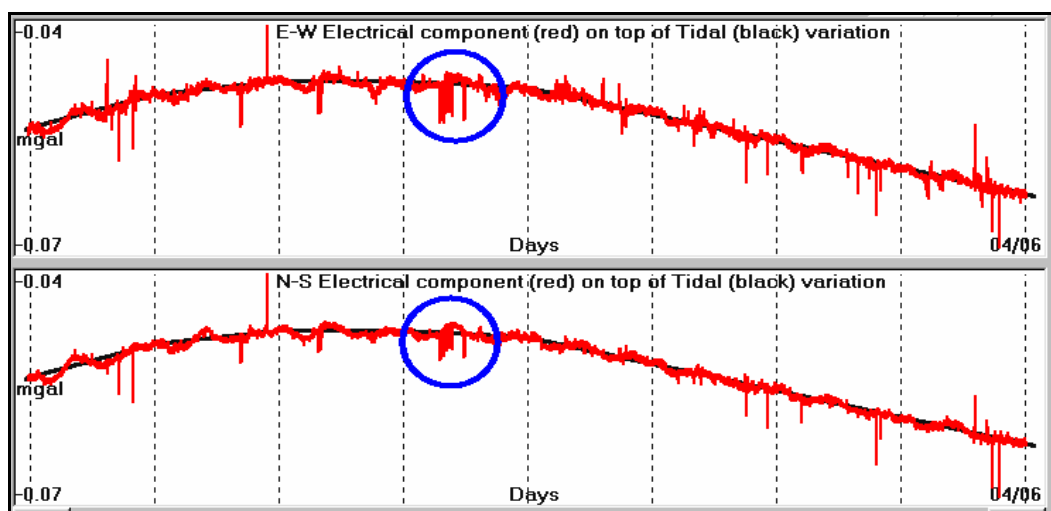


Fig. 4.1.10.9. **SES** precursory, electrical signal (in blue circles) recorded, by **HIO** monitoring site, during the 30th May 2006 (HIO060530).

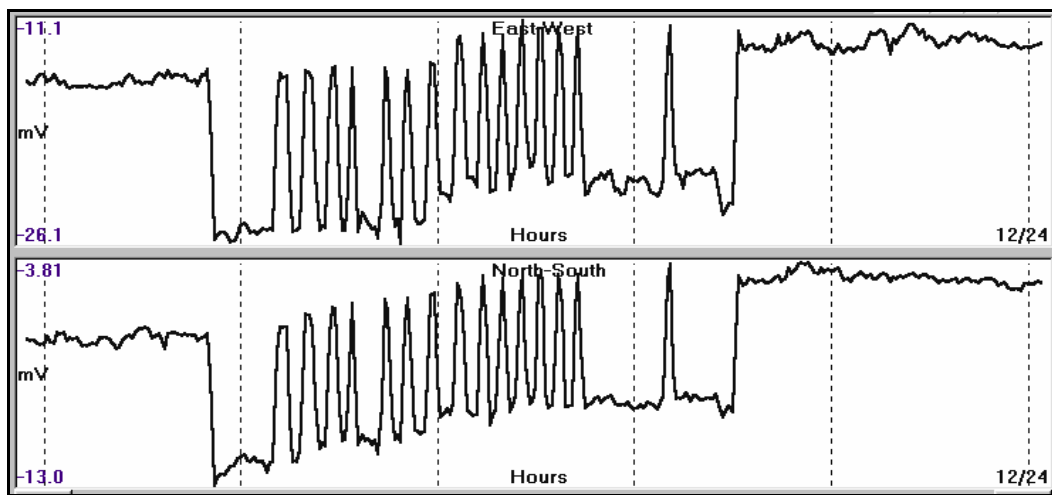


Fig. 4.1.10.9.a. Zoom-in of the SES signal of fig. (4.1.10.9).

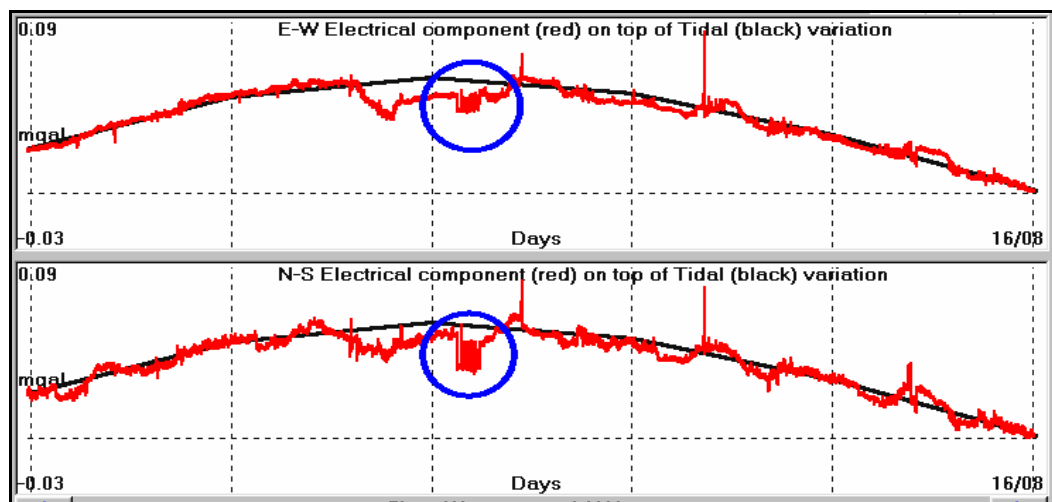


Fig. 4.1.10.10. **SES** precursory, electrical signal recorded, by **HIO** monitoring site on 13th August 2006 (HIO060813).

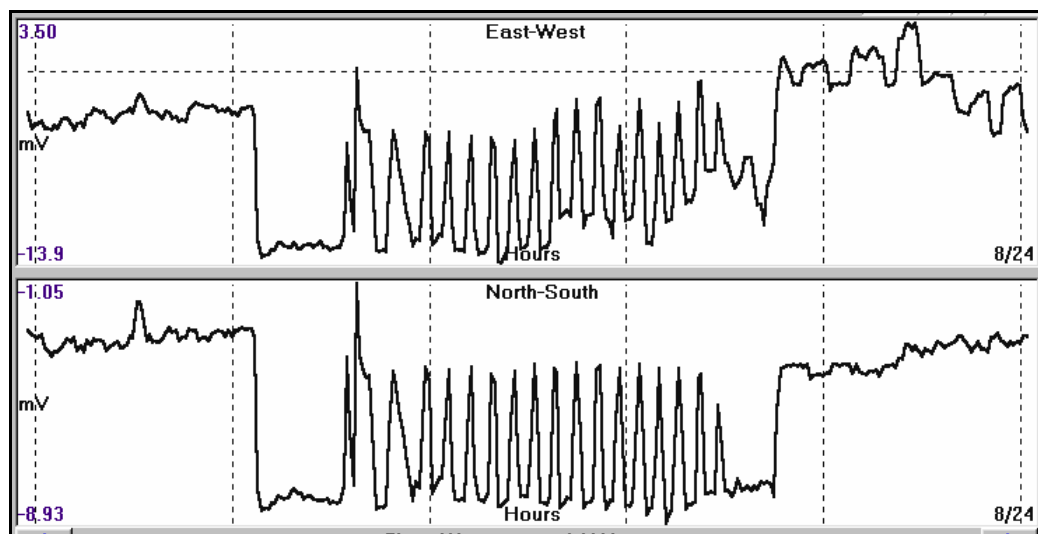


Fig. 4.1.10.10.a. Zoom-in of the **SES** signal of fig. (4.1.10.10).

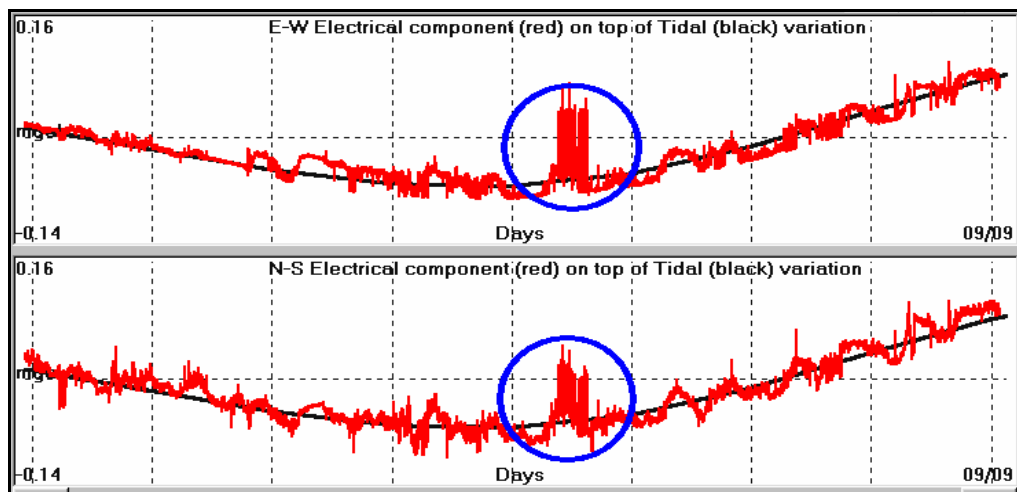


Fig. 4.1.10.11. **SES** precursory electrical signal (in blue circles) recorded by **HIO** monitoring site, on 5th September 2006 (HIO060905).

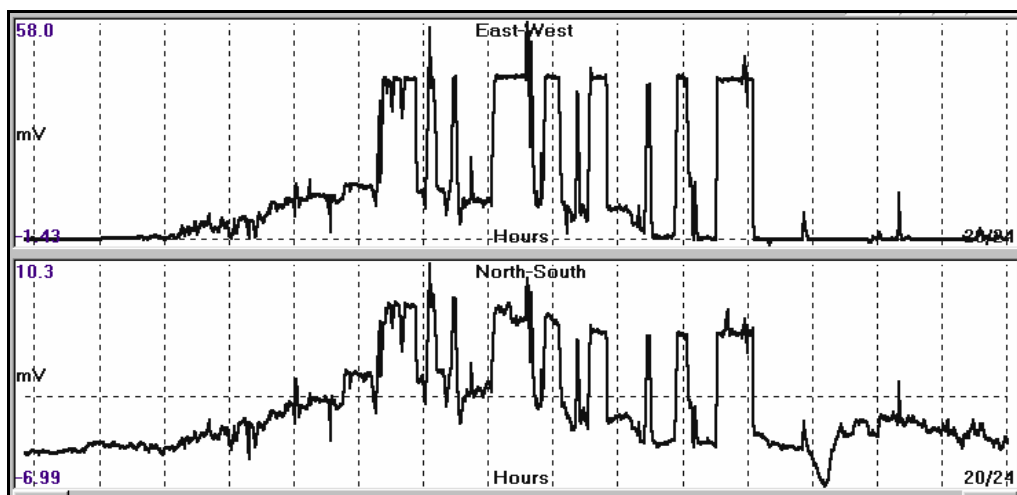


Fig. 4.1.10.11.a. Zoom-in of the **SES** signal of fig. (4.1.10.11).

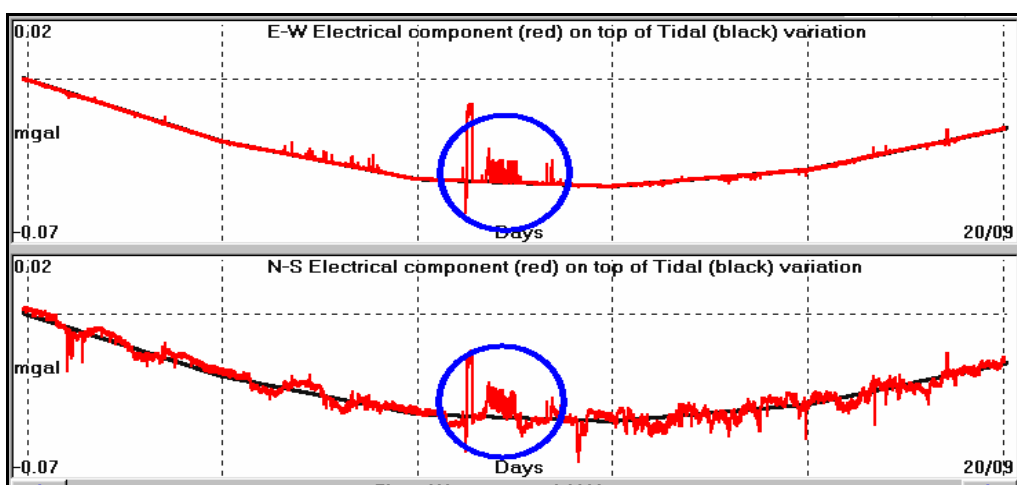


Fig. 4.1.10.12. **SES** precursory, electrical signal (in blue circles) recorded, by **HIO** monitoring site on 17th September 2006 (HIO060917).

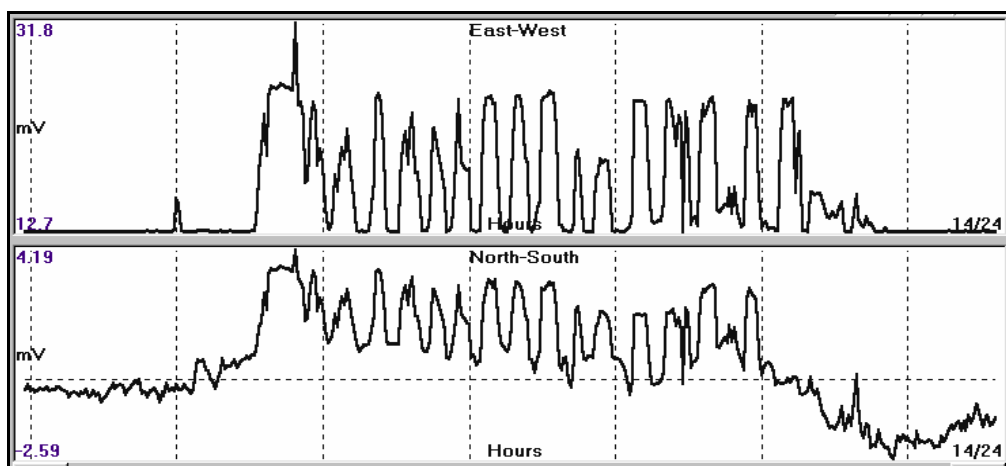


Fig. 4.1.10.12.a. Zoom-in of the **SES** signal of fig. (4.1.10.12).

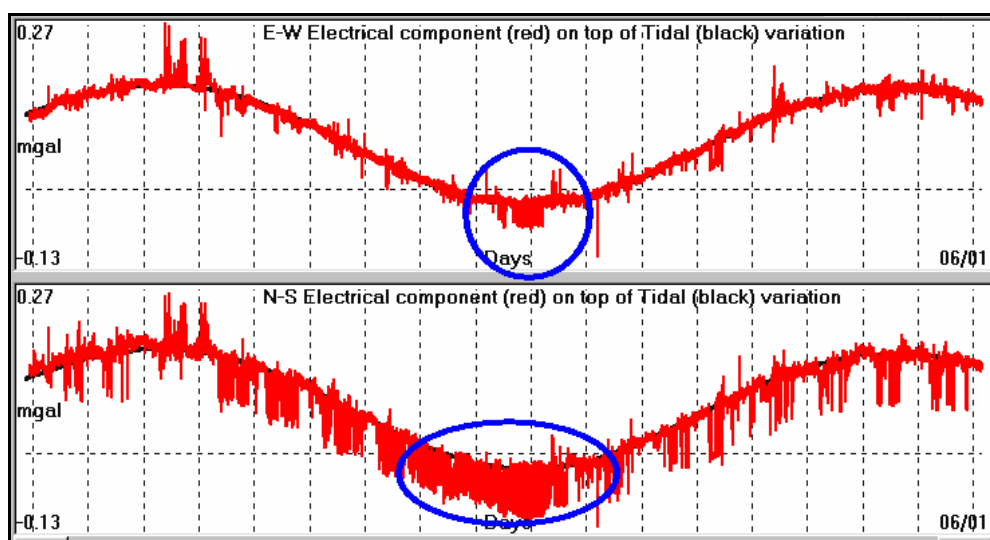


Fig. 4.1.10.13. **SES** precursory, electrical signal (in blue circles) recorded, by **HIO** monitoring site, on 28th December 2006 (HIO061228).

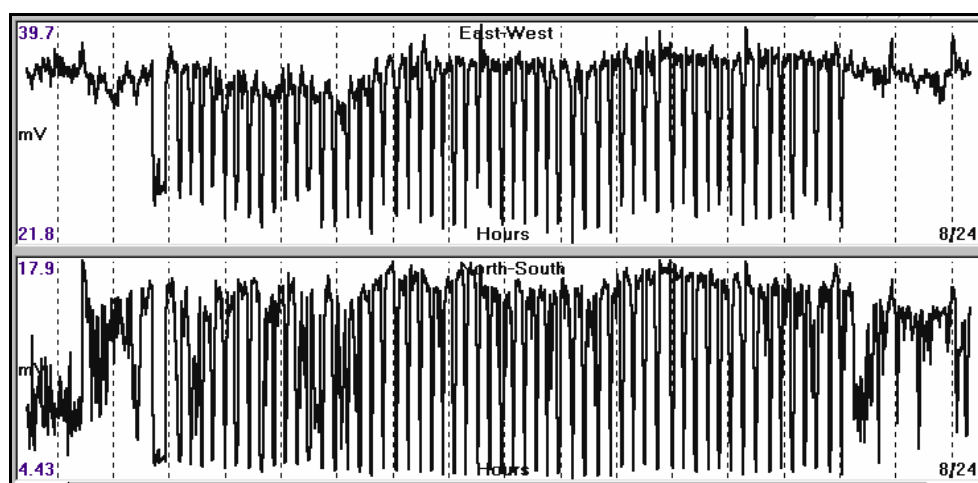


Fig. 4.1.10.13.a. Zoom-in of the **SES** signal of fig. (4.1.10.13).

SES signals recorded at PYR monitoring site, compared to 14 days period, tidal lithospheric oscillation.

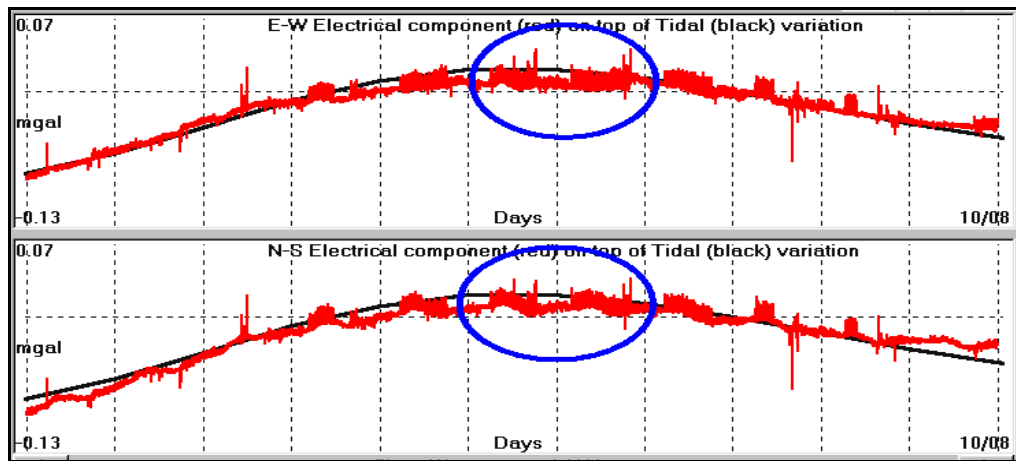


Fig. 4.1.10.14. **SES** precursory, electrical signal recorded, by **PYR** monitoring site, on 4th August 2004 (PYR040804).

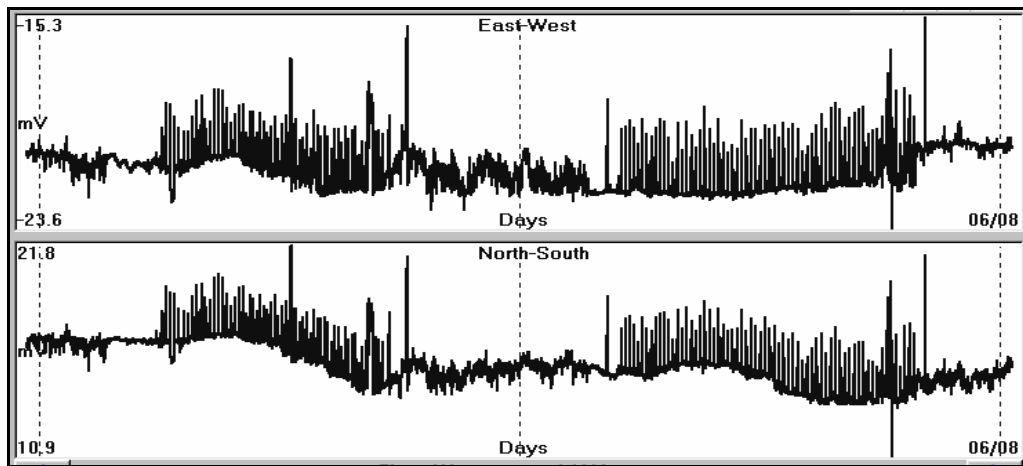


Fig. 4.1.10.14.a. Zoom-in of the (4th - 5th of August) **SES** signal of figure (4.1.10.14).

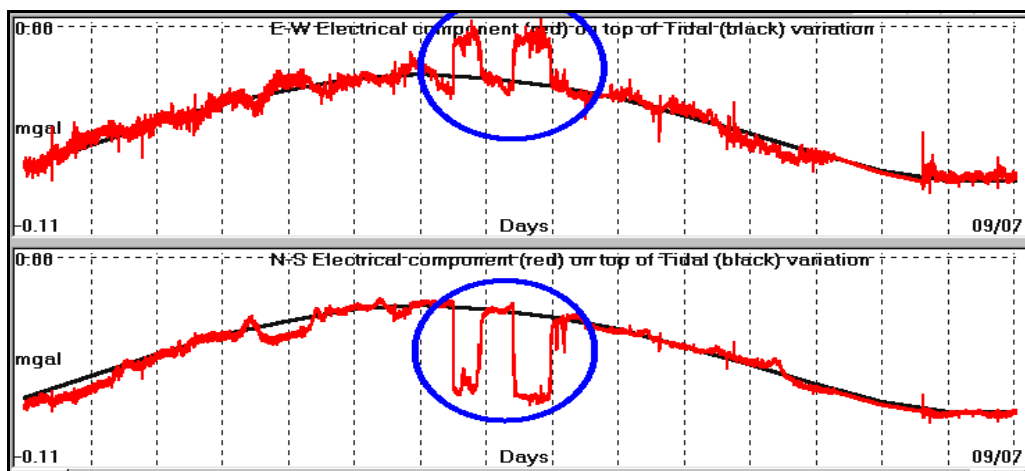


Fig. 4.1.10.15. **SES** precursory, electrical signal recorded, by **PYR** monitoring site, on 30th June, 2006 (PYR060630).

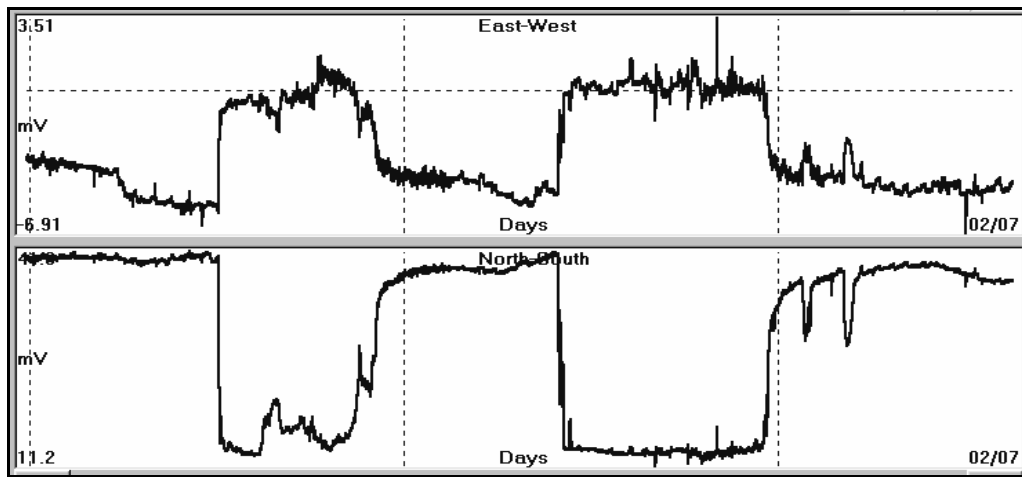


Fig. 4.1.10.15.a. Zoom-in of the **SES** signal of figure (4.1.10.15).

SES signals, recorded, by ATH monitoring site, compared, to 14 days period, tidal lithospheric oscillation.

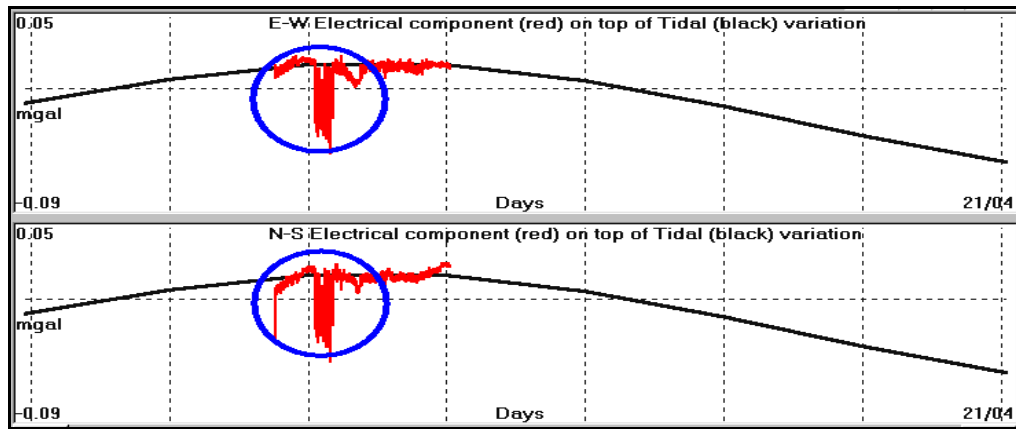


Fig. 4.1.10.16. **SES** precursory, electrical signal recorded, by **ATH** monitoring site, on 16th April, 2003 (ATH030416).

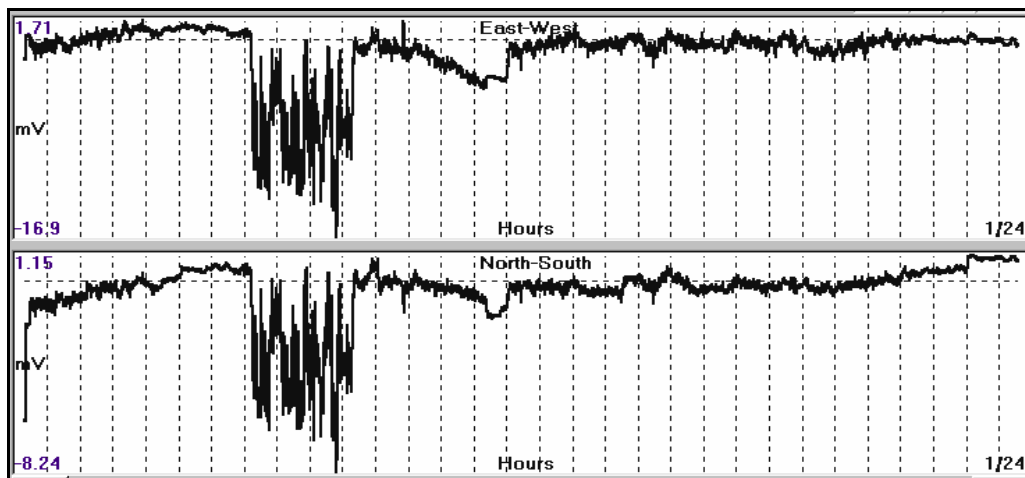


Fig. 4.1.10.16.a. Zoom-in of the SES signal of figure (4.1.10.16).

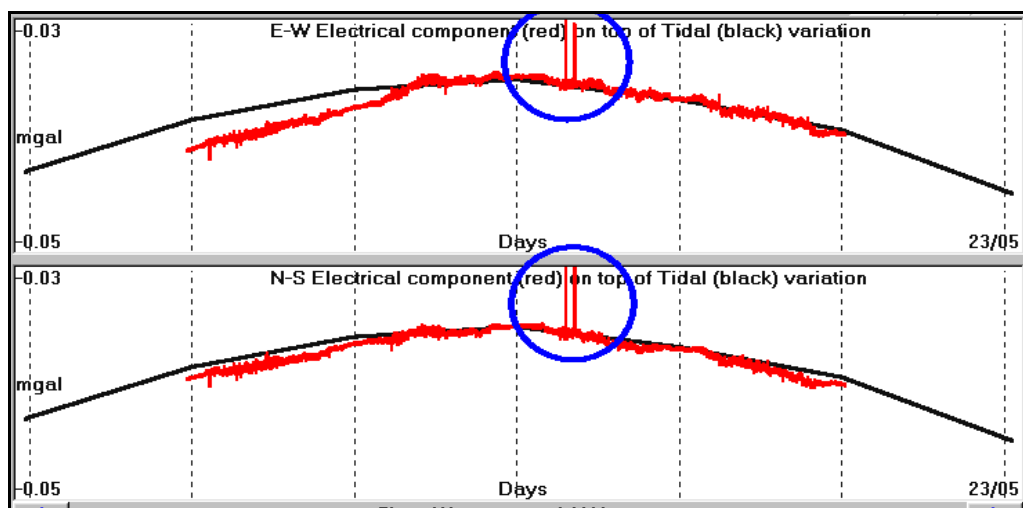


Fig. 4.1.10.17. **SES** precursory, electrical signal recorded, by **ATH** monitoring site, on 20th May, 2004 (ATH040520).

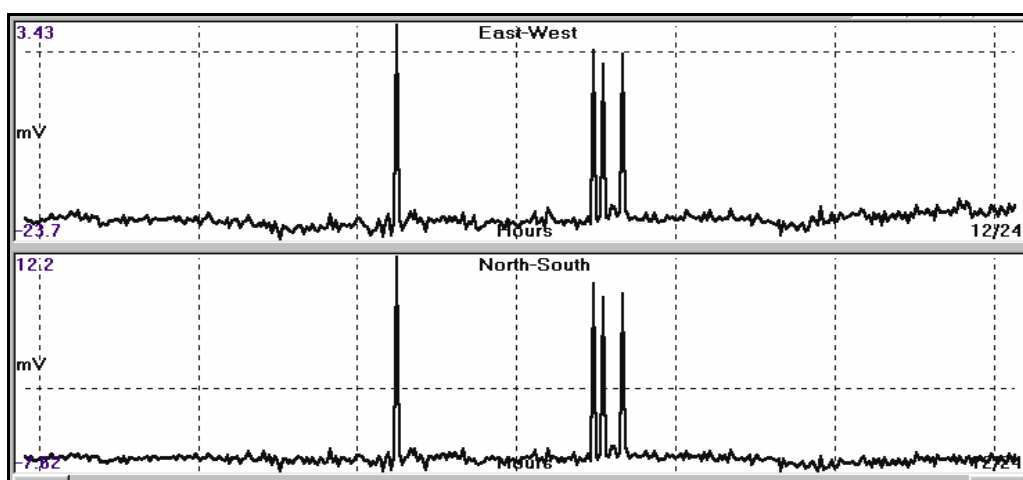


Fig. 4.1.10.17.a. Zoom-in of the SES signal of figure (4.1.10.17).

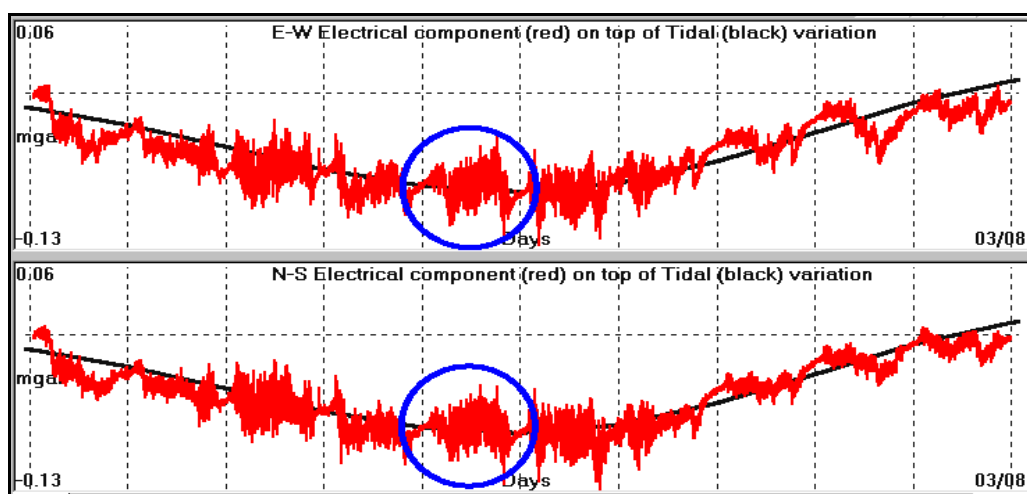


Fig. 4.1.10.18. **SES** precursory, electrical signal recorded, by **ATH** monitoring site, on 29th July, 2004 (ATH040729).

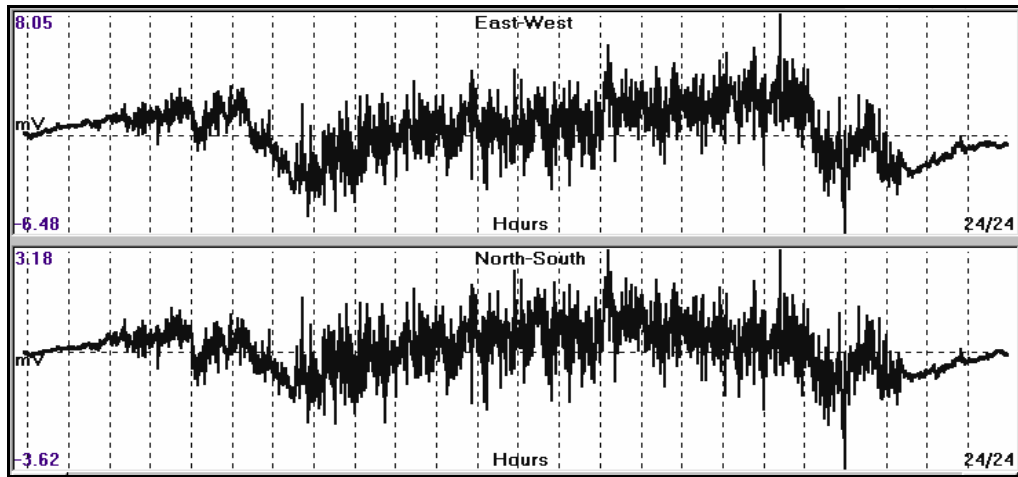


Fig. 4.1.10.18.a. Zoom-in of the SES signal of figure (4.1.10.18).

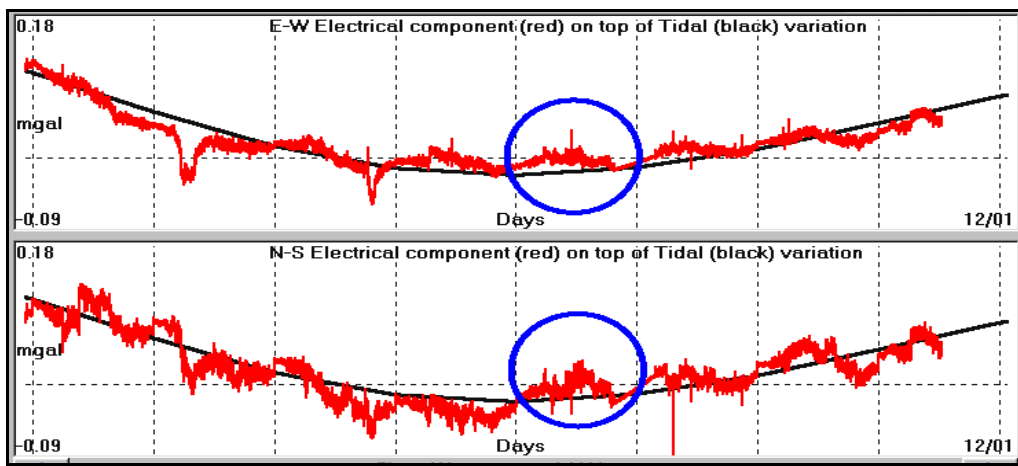


Fig. 4.1.10.19. **SES** precursory, electrical signal recorded, by **ATH** monitoring site, on 8th January, 2006 (ATH060108 EQ6.9).

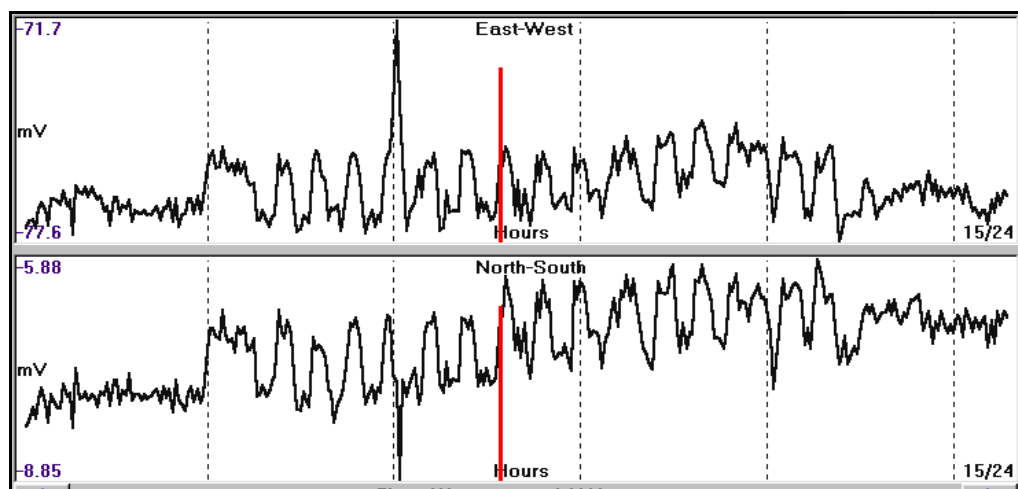


Fig. 4.1.10.19.a. **SES** precursory, electrical signal recorded, by **ATH** monitoring site, on 8th January, 2006 (ATH060108 EQ6.9). The red bar indicates the time of occurrence of the 6.9R EQ (ATH060108 EQ6.9).

The previous figures (4.1.10.19 - 4.1.10.19.a) indicated the close correlation of the EQ time of occurrence, to the 14days tidal, lithospheric oscillation peak time and the present "coseismic" **SES** signal.

It developed almost 90 minutes before the EQ occurrence and vanished, almost 110 minutes after it. This suggests that, the catastrophic deformation of the seismogenic area is estimated to have lasted for about 3 hours.

In literature, and specifically in the papers which were published by the **VAN** group during their research activity, a lot of **SES** signals have been presented. It is worth to test the time (day) of occurrence of these signals against the tidal lithospheric oscillation of the 14 days period. To this end, the already published signals which were traceable (**No = 64**), are tabulated in **Table - 2**. The first column indicates the time of occurrence of the **SES** in yyyyymmdd format, while the second one indicates the time lag, between the **SES** times considered as "zero" time and the time of the tidal peak value.

TABLE - 2

SES date (yyyyymmdd)	Tidal peak lag (days)	SES date (yyyyymmdd)	Tidal peak lag (days)
19810707	-2	19850514	-2
19810923	0	19850516	3
19810924	0	19880401	0
19810927	-4	19880515	1
19810929	2	19880831	-1
19810930	1	19880831	0
19811001	0	19880929	-1
19811219	0	19881003	2
19820118	0	19891018	-1
19830115	0	19900426	-1
19830118	-2	19930127	-3
19830130	0	19930224	-2
19830131	-1	19930224	-2
19830202	-3	19950406	2
19830217	-3	19950418	-1
19830607	-1	19950418	-1
19830614	-1	19950419	3
19830704	2	19950430	0
19830711	1	19950513	2
19831007	1	19950917	2
19831010	-1	19980621	-1
19840123	2	19980814	-2
19840207	-3	19990901	-1
19840208	-2	19990902	-2
19840219	-1	19990906	0
19840504	-3	19990907	0
19840508	0	20010317	0
19840514	0	20010725	-1
19840515	0	20040514	-2
19841114	-2	20050321	3
19850412	0	20050407	0
19850430	-1	20060323	0

The negative values, of the second column, indicate that the **SES** time of occurrence follows the tidal peak", while the positive values indicate that the **SES** "preceded the corresponding, tidal peak".

The values, tabulated, in table (2), are presented in a graph form, in the following figure (4.1.10.21).

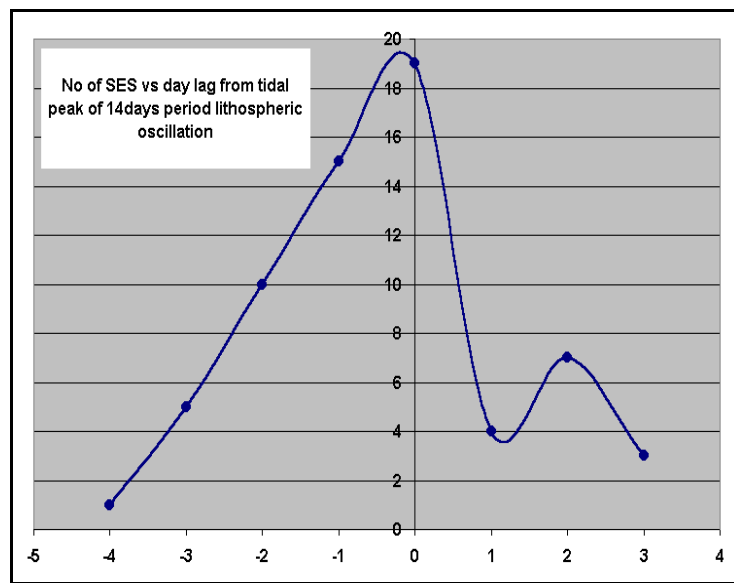


Fig. 4.1.10.21. Number of **SES**, as a function of time lag to tidal peak of the 14 days lithospheric oscillation are, presented.

The form of the function of **SES** time vs. time lag to tidal oscillation peak times suggests that the majority of the **SES** occur at some time “following” the tidal peak occurrence. By taking into account that the stress-strain charge of the lithosphere is at maximum load conditions during peak tidal oscillating values, then it is justified to accept that the majority of **SES** are generated in “decompression conditions” or in other words **SES** are “**pressure stimulated depolarization currents - PSDC**” (Varotsos, 2005).

The stress-strain charge conditions where an **SES** may develop are steps of sudden increase or decrease of the stress-strain load of the lithosphere. It is worth to compare such stress-strain changes in the lithosphere, during the preparation phases of an earthquake. Firstly, is considered the model, proposed, by Mjachkin et al. (1975). In this model (fig. 4.1.10.22), three characteristic phases are present, concerning the deformation velocity during a seismic cycle. In the first (I) phase, the seismogenic area exhibits homogeneous cracking; during the second (II) phase, cracking acceleration, due to interaction of cracks, is exhibited; and during the third (III) phase, unstable cracking and main fault formation is exhibited, and the generation of the main, seismic event follows.

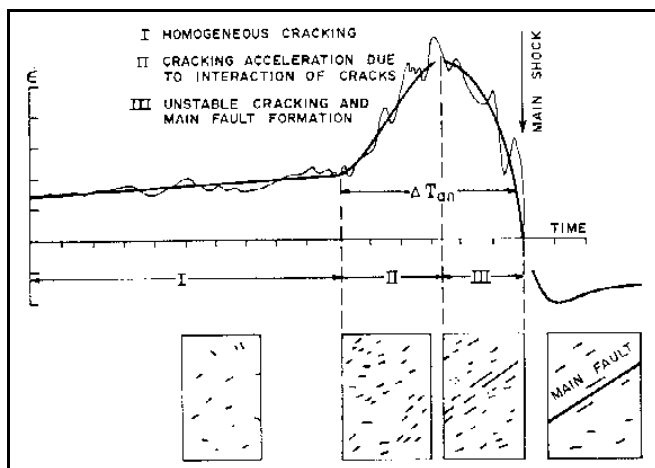


Fig. 4.1.10.22. Change of average deformation velocity, during the seismic cycle (Mjachkin et al. 1975).

Change of stress-strain load, which can cause the generation of **SES**, occurs in the boundaries between phases (I) and two (II), between phases (II) and (III) and very shortly before the main, seismic event. The time span of each phase is generally unknown and therefore, even if the SES has been observed, the time window of occurrence of the pending seismic event, is still highly unpredictable.

The piezoelectric model will be considered next. There are two distinct regions, where non-linear change of the strain load exists in the strain-stress curve. In area (A), there is a rapid non-linear increase of the strain, while in area (B), there is a non-linear decrease of the strain. These are favorable areas, where **SES** can develop either as **PSPC** or as **PSDC**.

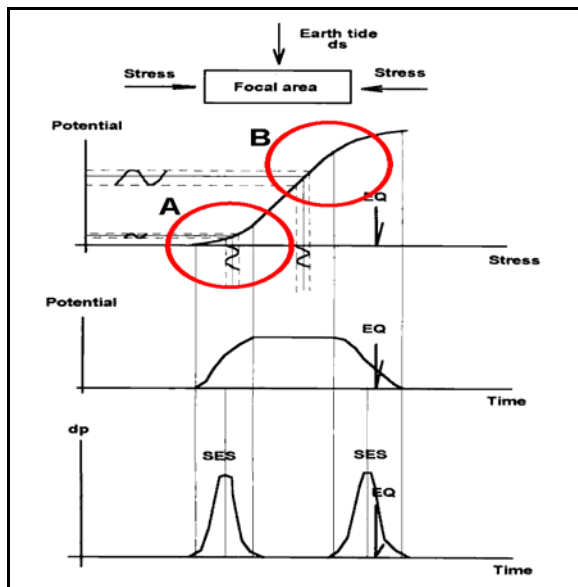


Fig. 4.1.10.23. Areas of “compressional (A) stress - strain increase” and “decompressional (B) stress - strain decrease”.

These signals can be considered as of higher order derivatives of the total piezoelectric potential generated, in terms of the function of Piezoelectric Potential vs Time / Stress load. The timing problem of an earthquake still exists, since the time interval between areas (A) and (B), is still unknown.

A search, in the **VAN** group literature, indicates that the time of occurrence of an **SES** may precede the time of occurrence of the corresponding earthquake, from **30-240 minutes** (papers of 1981) up to **11 days** (papers of 1993) and probably of longer periods. The latter is not surprising, if it is explained by the tidal lithospheric oscillation. Actually, an **SES** can be generated at any favorable tidal oscillation peak value, but the corresponding earthquake will occur later on, when its critical stress-strain conditions are met at a specific, future, tidal oscillation peak.

No matter what their origin is, what is important is the fact that such signals are composed by series of short pulses in the form of “train pulses”. A physical mechanism which can produce signals of this kind is postulated as follows:

Let us consider the very tiny rock element, which exhibits the rock properties of the seismogenic region. It is assumed that, this basic element follows the stress-strain charge conditions of the entire seismogenic area. During the boundaries of the different phases of the Mjachkin et al. (1975) model or the areas (A) and (B) of the piezoelectric model, this basic rock element undergoes, firstly, a stress-strain increase, which is followed, in very short time, by a decrease of stress-strain and fracturing, thus creating the acceleration of cracking. Therefore, this basic rock formation element is capable to produce, initially, a tiny **PSPC**, which is followed by a **PSDC** before its final fracture.

Moreover, electrical signals of the same amplitude, but of different polarity, depending on the polarity (increase or decrease) of the stress-strain rate for the same basic rock element and for the same rate of stress-strain charge-discharge, will be generated. Therefore, **each pair**

of positive-negative current pulses, generates a “square electrical, potential pulse”, the basic element of the “train pulse”, which exhibits a duration of a few minutes, which depends on the time, required, to complete its “tiny seismic cycle”.

The close inspection of the **SES** signals, recorded by **ATH**, **PYR** and **HIO** so far, indicates that a period of 8-15 minutes, but shorter periods as well (from a few ms to a few minutes) have been recorded by the **VAN** group.

Summarizing all the above, it can be said that, the **SES** presence is a clear indication that an unknown seismogenic area has reached a stress-strain level, close, to the critical stress-strain charge conditions, which are necessary for the generation of a seismic event. The problem that still exists, in terms of “time prediction”, is that, **there is no method (in terms of short-term prediction), to suggest the calculation of the time to remain between the SES occurrence and the time of the seismic event. When this seismic event will occur, is still unknown.**

b. Oscillatory type earthquake precursory signals.

The uncertainty for the timing of a future seismic event, which is introduced: a) by the use of **SES**, as it was explained earlier, b) by the use of Mjachkin et al. (1975) fracturing model and c) by the piezoelectric model (see **fig. 4.1.10.23**) is resolved, in most cases, by the study of the oscillatory component of the Earth’s electric field. This type of component is induced by the lithospheric plate tidal oscillation; see Section (3) and the piezoelectric model of figure (4.1.10.23). An increase in amplitude of the Earth’s oscillating, electric field develops and lasts all along the time between the two regions (A) and (B). Shortly after the (B) area, the seismic event takes place. Consequently, the presence of this type of oscillation indicates that the seismogenic area has passed the (A) area and approaches the (B) one, in a short time. The seismic event occurs at the next tidal amplitude peak, of the 14 days period, tidal, lithospheric oscillation, when the stress-strain load is at its maximum (Thanassoulas et al. 2003). Samples of such oscillations, along with the corresponding earthquakes that occurred at the tidal oscillation peak, are presented in the following figures:

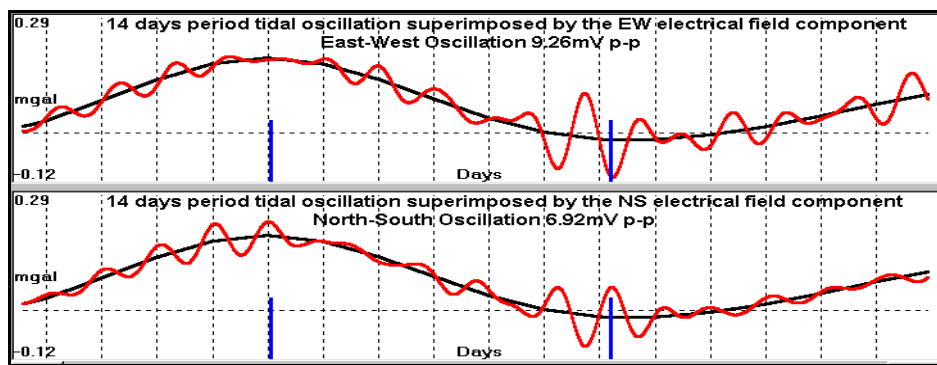


Fig. 4.1.10.24 Daily tidal oscillation of the earth’s electric field (red line on top of the 14 days period, tidal, lithospheric oscillation – black line, **VOL** monitoring site). The blue bars indicate the time of occurrence of two earthquakes of $M = 4.8R$ (Thanassoulas et al. 2003)

In the first example of figure (4.1.10.24) it is evident that the two earthquakes of $M = 4.8R$, which occurred in the presented period of 16 days (1st January, 2001 – 17th January, 2001), took place exactly on the day of the peak of the 14 days period, tidal, lithospheric oscillation.

Moreover, both earthquakes were preceded by an increase of the amplitude of the electric field oscillation.

In the next example (**fig. 4.1.10.25**) the presented time period spans from 22nd April, 2001 to 1st May, 2001. The only one earthquake of magnitude $M = 5.3R$, which took place in this period, occurred on the peak of the 14 days period of the tidal lithospheric oscillation.

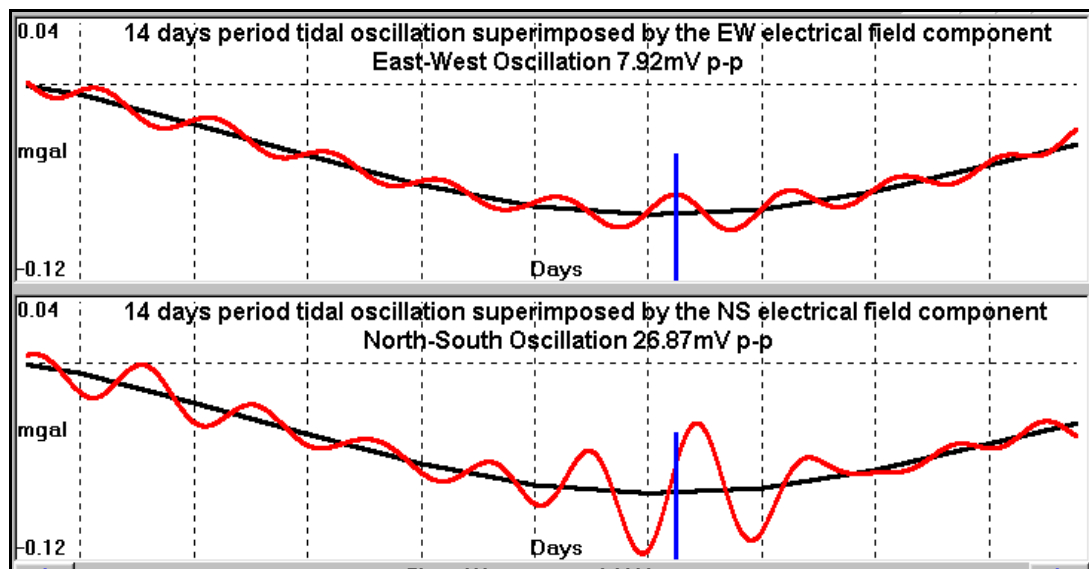


Fig. 4.1.10.25. Daily tidal oscillation (22nd April to 1st May, 2001) of the Earth's electric field (red line on top of 14 days period, tidal, lithospheric oscillation – black line, **VOL** monitoring site). The blue bar indicates the time of occurrence of the M = 5.3R earthquake (Thanassoulas et al. 2003).

In the next case (**fig. 4.1.10.26**), which corresponds to the period of 11th August, 2002 to 4th September, 2002, three consecutive earthquakes of M = 5.1R occurred, during the peak value of the 14 days period, tidal, lithospheric oscillation.

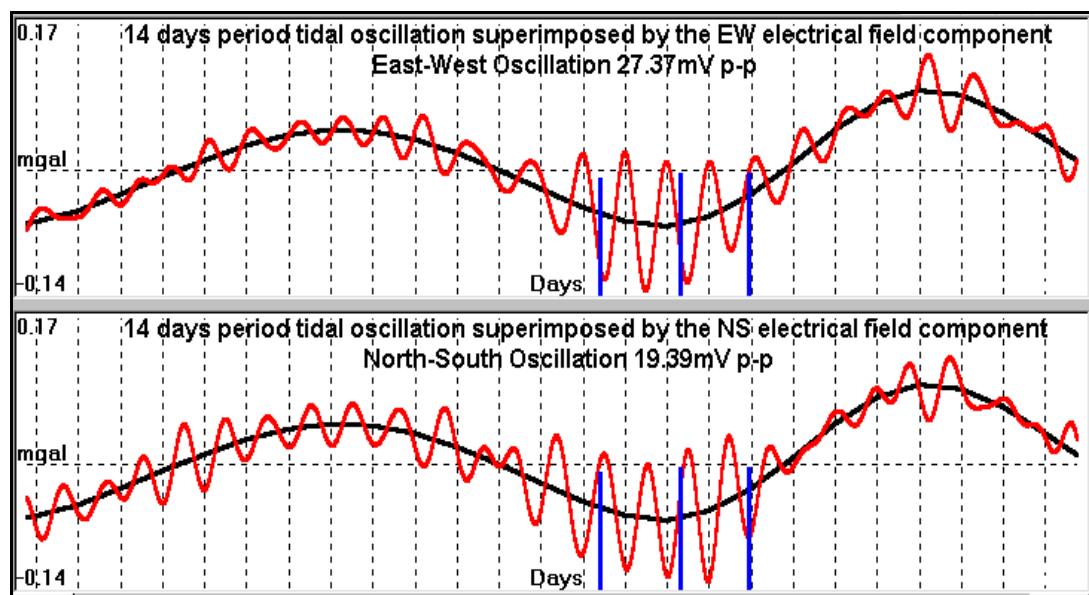


Fig. 4.1.10.26. Daily tidal oscillation (11th August to 4th September 2002) of the Earth's electric field (red line on top of 14 days period, tidal, lithospheric oscillation – black line, **VOL** monitoring site). The blue bars indicate the time of occurrence of three earthquakes of M = 5.1R (Thanassoulas et al. 2003).

One more example is presented in the following figure (**4.1.10.27**). In a month's period (15th June to 13th July, 2003) one earthquake occurred, 3 days after the peak value of the 14 days period, tidal, lithospheric oscillation. That earthquake was preceded by an increase of the amplitude of the Earth's daily oscillation of its electric field.

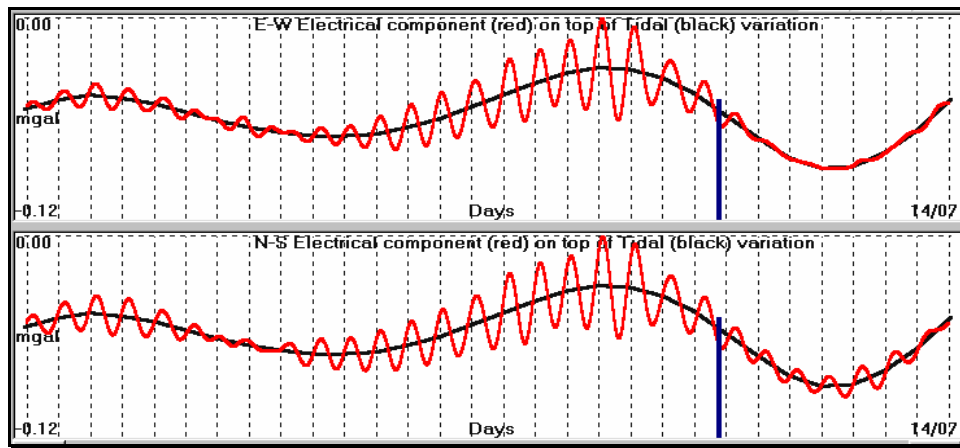


Fig. 4.10.27. Daily tidal oscillation (15th June to 13th July, 2003 red line, **PYR** monitoring site) of the Earth's electric field on top of 14 days period, tidal, lithospheric oscillation (smoothly oscillating black line). The blue bar indicates the time of occurrence of the $M = 5.5R$ earthquake.

An exceptional example is the one in figure (4.1.10.28). This example presents Skyros earthquake case ($M = 6.1R$, 26th July 2001). The main seismic event was preceded by a drastic increase of the amplitude of the Earth's electric, daily oscillating field, which lasted for a few days. On 23rd July the data were presented in the seminar organized by the **INRNE**, **BAS**, Bulgaria and following this methodology, it was suggested (a priori), that this earthquake is likely to happen on 25th to 26th July (after 2 days) and specifically **20 minutes to midnight (GMT)**.

It was, obviously, a very strong statement, taking into account that, in the best case, the seismological community accepts "predictive capability" for medium term predictions only.

What followed the next two days is what was exactly expected to happen, always according to the already, proposed, methodology. The earthquake **took place 20 minutes after midnight**. The proof of this fact is presented in the following figures. In figure (4.1.10.28) is presented the 14days tidal, lithospheric oscillation, superimposed by the daily, oscillating Earth's electric field.

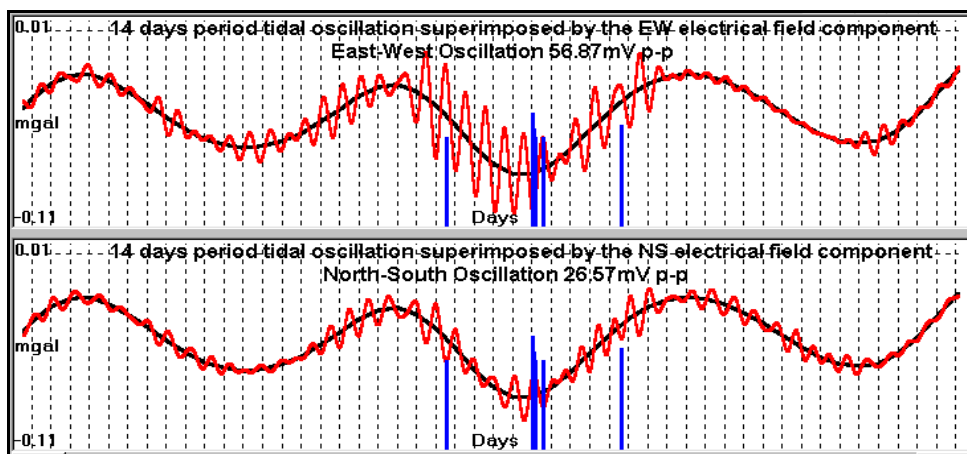


Fig. 4.1.10.28. Skyros EQ (26th July 2001). Fore – main - after shocks are indicated by blue bars. 14 days tidal lithospheric oscillation is represented by a smooth black line, while the red line indicates the daily oscillating Earth's electric field (Thanassoulas et al. 2003).

The main event took place at the minimum peak of the 14 days, tidal, lithospheric oscillation (fig. 4.1.10.29), while, during this 14 days period peak tidal value, there was, simultaneously, a daily tidal peak value, at the time "**20 minutes to midnight of 25/26th of July**". Therefore, following the methodology, which had already been presented, the pending earthquake, would take place, due to the presence of the generated, strong, electrical signals:

a) at the peak of the 14 days period, tidal, lithospheric oscillation, thus suggesting the date 25th to 26th (**fig. 4.1.10.29**)

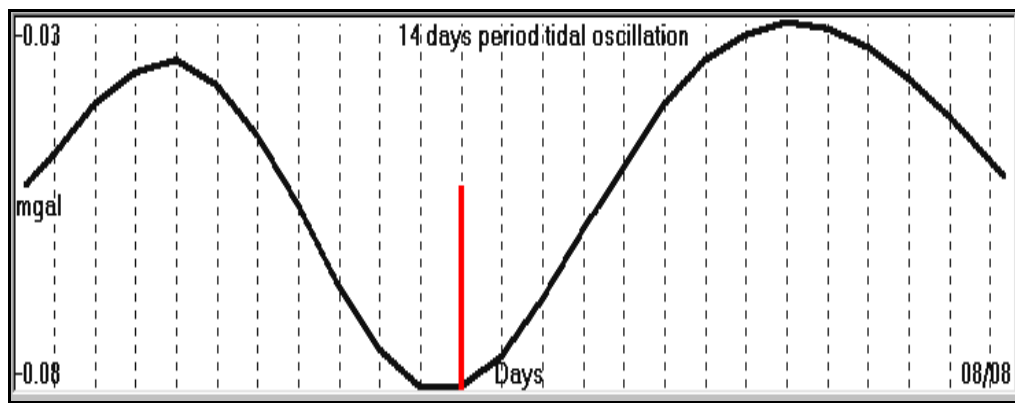


Fig. 4.1.10.29. Skyros EQ (26th July 2001, $M = 6.1R$) time of occurrence (red bar), correlated, to the 14 days period, tidal, lithospheric oscillation (Thanassoulas et al. 2001b).

b) 20 minutes to midnight (**fig. 4.1.10.30**).

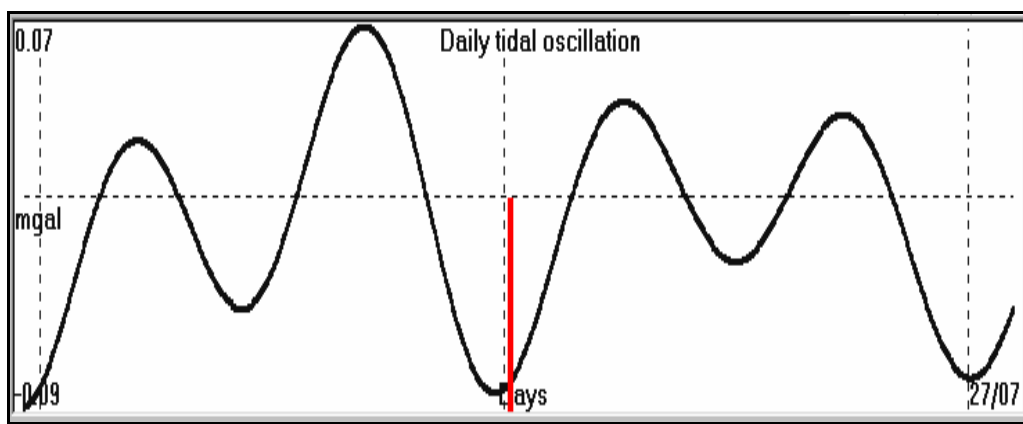


Fig. 4.1.10.30. Skyros EQ (26th July 2001, $M = 6.1R$) time of occurrence (red bar), correlated, to the daily, tidal, lithospheric oscillation (Thanassoulas et al. 2001b).

It is anticipated that for a scientist, initially, it is very difficult to believe this prediction. In order to resolve this unpleasant situation it was asked from the BAS organizing committee, to validate it, in written form. The produced validation is presented in the following page.

Seminar Conclusions

On the 23rd of July, 2001 a 3-day seminar was held in INRNE, Bulgarian Academy of Sciences, Sofia, Bulgaria, titled:

"The possible correlation between electromagnetic earth surface fields and future earthquakes."

During this seminar, Assoc. Prof. Ranguelov, B., seismologist, Assoc. Prof. Mavrodiev, S. Theor. Phys. and Dr. Thanassoulas, C., Geophysicist presented their research results on the seminar topic.

Furthermore the aim of the seminar was to investigate the possibilities for submission of a common research program, to establish a regional network for monitoring different geophysical parameters.

The presented examples of measurements of the earth's electric and geomagnetic fields indicate that it is possible to organize such type of a regional Balkan monitoring network for physical and geophysical fields that is going to permit the improvement of the earthquake prediction.

This was validated in practice by the occurrence, during this seminar, in Greece of a large earthquake ($M_s=6.1R$, 25/07/01) as it had been stated during the presentation of Dr. Thanassoulas and following the corresponding theoretical part of it (time determination), that could happen with very large probability. The magnetic observations, a few days before this large earthquake, presented unusual behavior too, with the specific daily variation of the 25th of July.

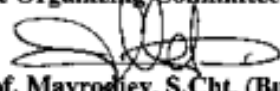
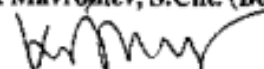
To this end the scientific community in Balkan region will be asked to collaborate into the implementation and submission of this project for funding by any appropriate authorities.

For easing the utilization of all the afore mentioned ideas the Organizing Committee proposes the foundation of a non government organization (NGO) under the title:

"The Balkans, Black Sea Region Sustainable Development (Harmonic Existence) and Science."



27 July, 2001
Sofia, Bulgaria

The Organizing Committee

Assoc. Prof. Mavrodiev, S.Cht. (Bulgaria)

Dr. Thanassoulas, Geophysicist (Greece)

Some more examples of earthquakes which were preceded by an increase of the Earth's daily oscillating field, recorded, by **PYR** monitoring site, are presented in the following figures:

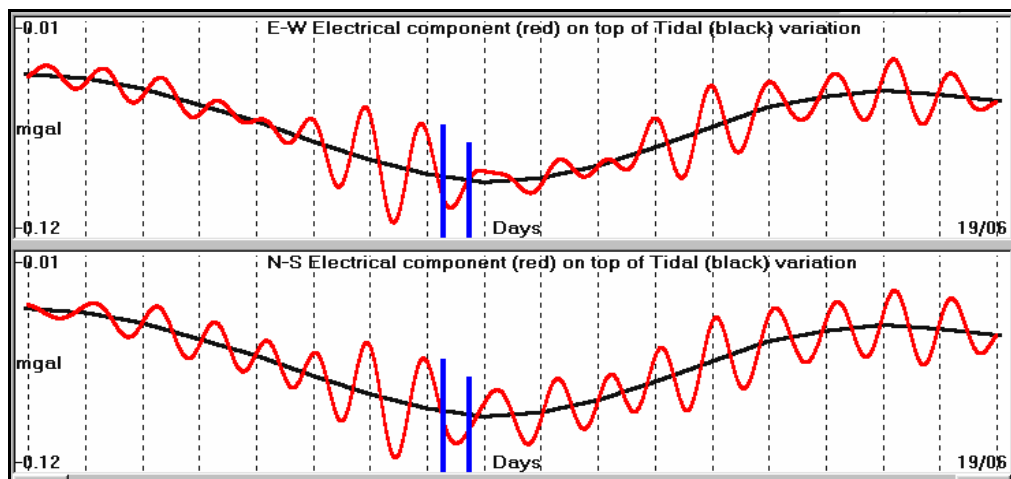


Fig. 4.1.10.31 Earthquakes ($M = 5R$, blue bars), which occurred one day before the 14 days period, tidal, lithospheric oscillation peak and were preceded by a daily, oscillating earthquake precursory signal. Recording period lasts from 2nd June to 18th June, 2003.

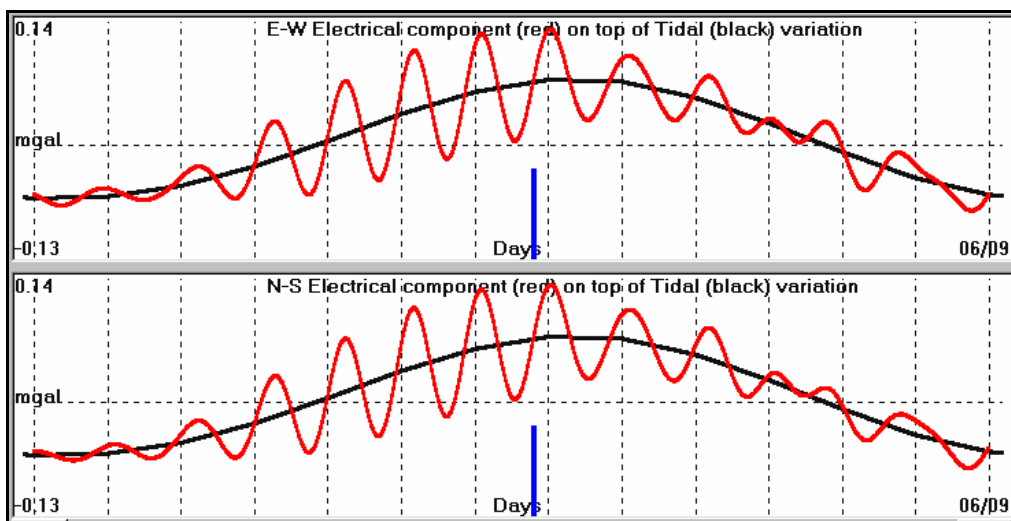


Fig. 4.1.10.32. Daily, tidal oscillation (24th August to 5th September 2003) of the Earth's electric field (rapid oscillation) on top of the 14 days period, tidal, lithospheric oscillation (smoothly, oscillating, black line). The blue bar indicates the time of occurrence of the $M = 4.8R$ earthquake.

Apart from the daily oscillating earthquake precursory signals, other types of signals, which precede strong earthquakes, have been observed, with much longer periods. These signals must conform to the lithospheric, oscillatory, tidal components, triggered, by the Sun – Moon interaction, upon the Earth. To date, the largest period of the oscillating Earth's electric field which has been observed, is that of 14 days. This electrical field oscillation conforms to the **M1** (Moon declination) tidal wave. Two such cases have been observed to date. The first one is the case of Lefkada, EQ (14th August, 2003, $M = 6.4R$) in Greece and the second is the Kythira, EQ (8th January, 2006 $M = 6.9R$) in Greece. These two cases are presented in the following figures:

In figure (4.1.10.33) is presented the oscillating Earth's electrical field with period of 14 days.

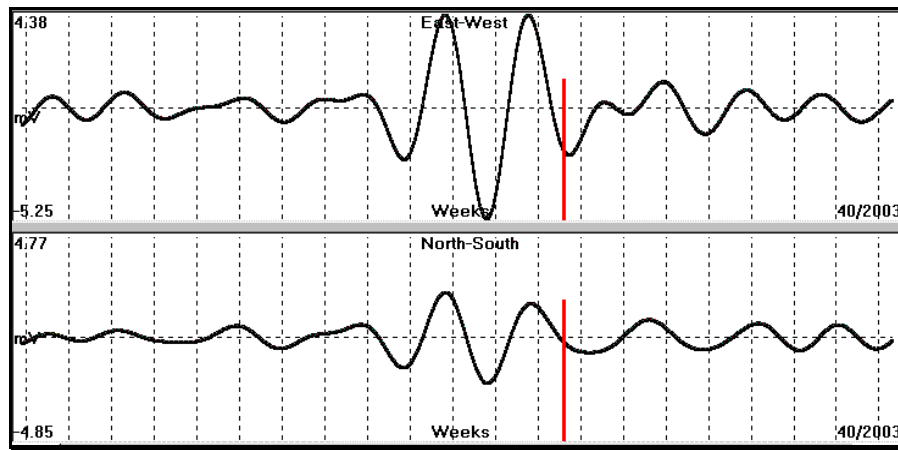


Fig. 4.1.10.33. 14 days period oscillating Earth's electric field observed prior to Lefkada, (14th August, 2003, M = 6.4R) earthquake in Greece. A red bar indicates the time of occurrence of this seismic event.

Next figure (4.1.10.34), represents the timing of the same seismic event in relation to the 14 days period, tidal, lithospheric oscillation. The EQ occurred 1 day before the next tidal peak.

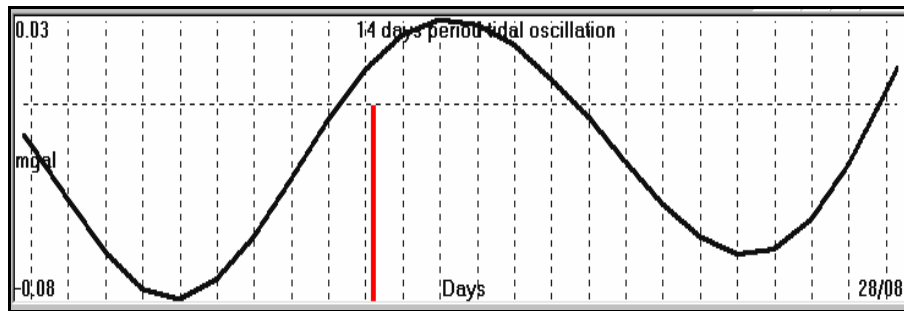


Fig. 4.1.10.34. Lefkada EQ (14th August 2003, M = 6.4R) time of occurrence (red bar), in relation to the 14 days period, tidal, lithospheric oscillation.

The very same seismic event occurred in the daily tidal minimum of the day of its occurrence, thus, validating its strong correlation to the tidal triggering mechanism of earthquakes.

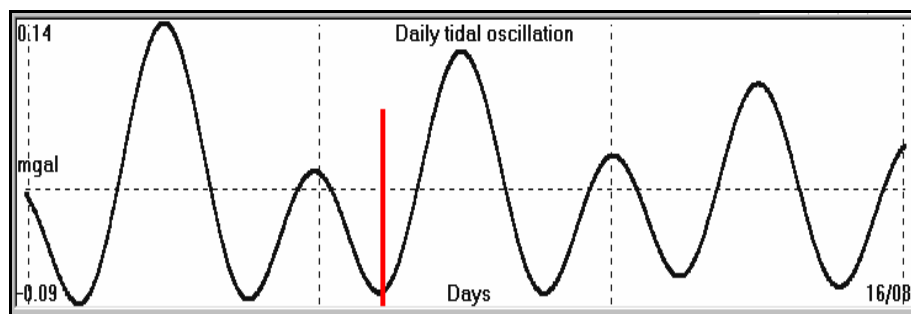


Fig. 4.1.10.35. Correlation of time of occurrence (red bar) of Lefkada, Greece EQ (14th August, 2003, M = 6.4R) to the daily, tidal, lithospheric oscillation.

Next example refers to Kythira earthquake (8th January, 2006, M = 6.9R). In figure (4.1.10.36) is presented the oscillating Earth's electrical field with period of 14 days.

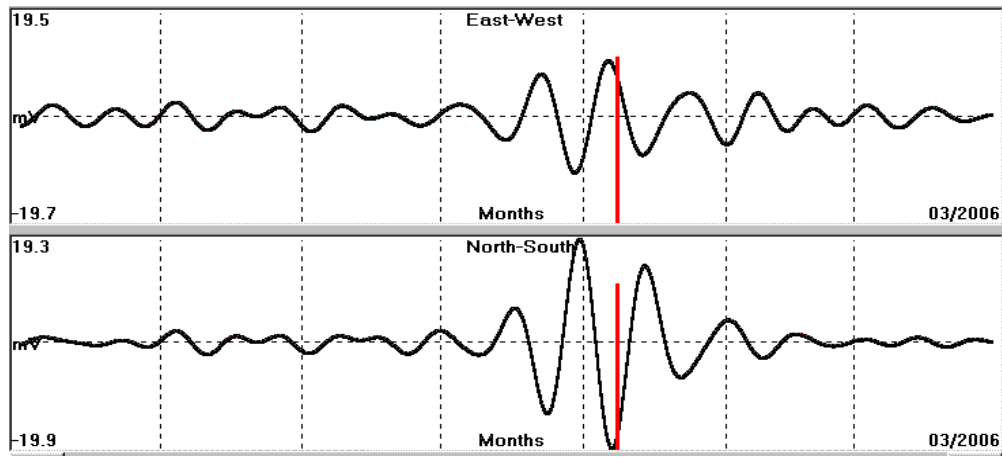


Fig. 4.1.10.36. 14 days period oscillating Earth's electric field, observed, prior to Kythira, (8th January, 2006, M = 6.9R) earthquake in Greece. A red bar indicates the time of occurrence of this seismic event.

Next figure (4.1.10.37), represents the timing of this seismic event, in relation to the 14 days period, tidal, lithospheric oscillation. The seismic event correlates quite well to the peak of the 14 days, tidal, lithospheric oscillation.

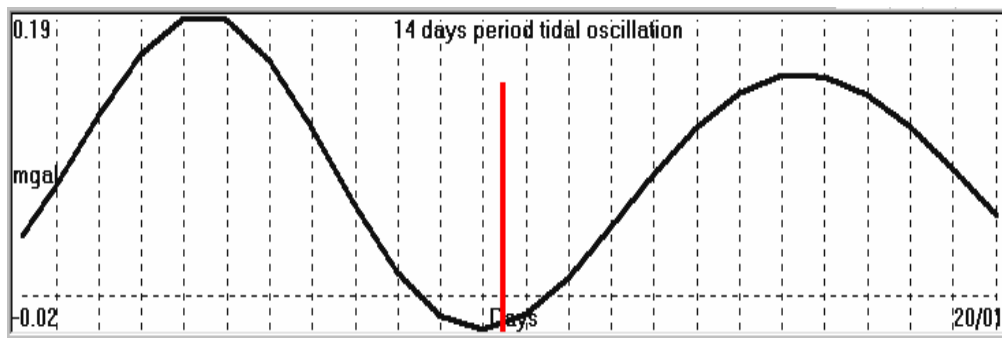


Fig. 4.1.10.37. Time of occurrence of Kythira EQ (red bar) is presented, in relation to the 14 days, tidal, lithospheric oscillation.

The comparison of the time of occurrence of Kythira EQ with the daily, tidal, lithospheric oscillation (fig. 4.1.10.38) indicates its very good fit to daily, tidal minimum.

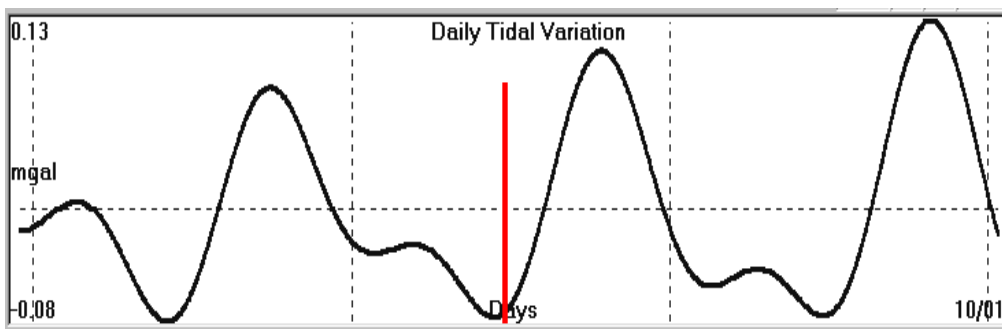


Fig. 4.1.10.38. Correlation of time of occurrence (red bar) of Kythira, EQ (8th January, 2006, M = 6.9R) in Greece, to the daily, tidal, lithospheric oscillation.

c. VLP signals

Very Long Period (**VLP**) earthquake precursory signals have been observed before strong earthquakes. Although, these signals cannot be correlated to the 14 days period, tidal, lithospheric oscillation, due to their very large “period”, they are warning indicators that “some regional, large, tectonic change” is going to take place. Whether this event ends up to a seismic event, depends on “shorter wave length” parameters. A representative sample of such a signal is presented in the following figure (4.1.10.40). It refers to Kythira EQ (8th January 2006, M = 6.9R), as it was recorded by Pyrgos (**PYR**) monitoring site. The recording covers (31) week’s period of time.

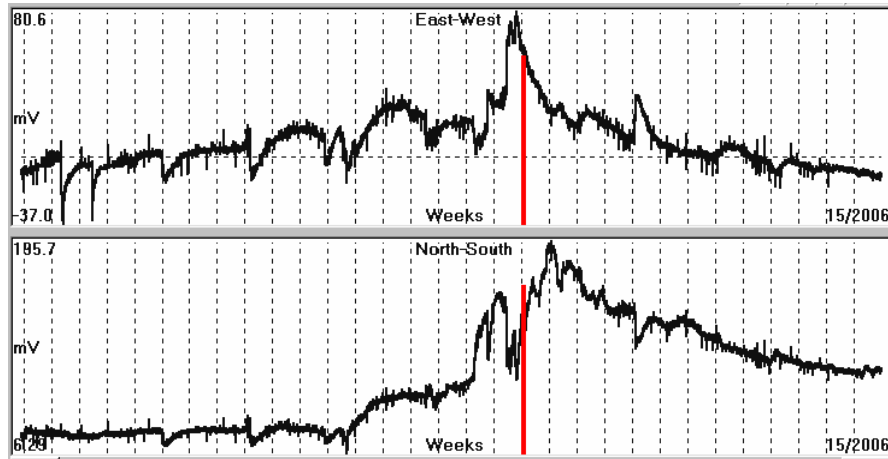


Fig. 4.1.10.40. Earth’s electric field recorded, for 31 weeks by **PYR** monitoring site. The time of the seismic (8th January 2006, M = 6.9R) event, is indicated by a red bar.

The rapid increase of its amplitude, before the seismic event, is more evident in the NS component. After the seismic event, the Earth’s electric field follows a slow decay, returning to its original level. As long as the EQ occurrence time gets closer, shorter period signals develop, which are reflected in both, recorded, components. A three weeks recording, before the seismic event, is shown in the following figure (4.1.10.41).

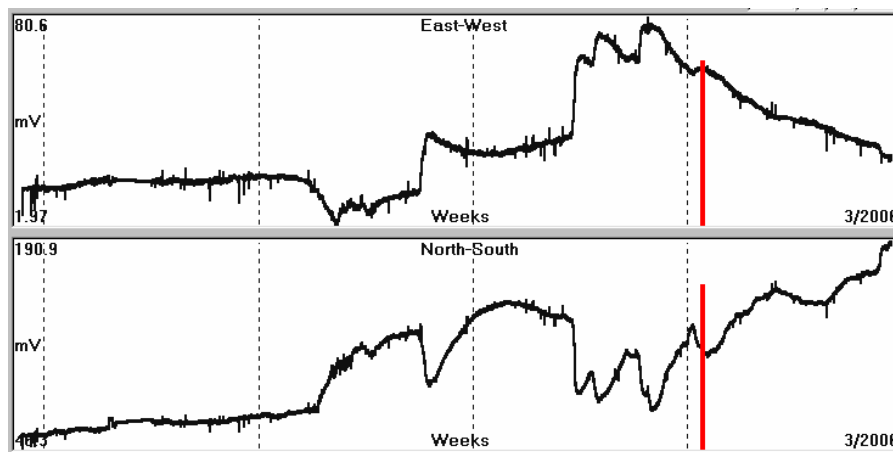


Fig. 4.1.10.41. A three weeks recording of the Earth’s electric field by **PYR** monitoring site, before the seismic event in Kythira (red bar).

The opposite polarity, observed between the two components (NS – EW), is explained from the azimuthal direction, observed, between PYR location and the epicentral area of Kythira EQ. The latter will be presented, in detail, in the section, which is referred to the “epicentral determination” of a strong EQ.

The fact that similar signals are observed even for a period of some days is not surprising. An example of such signals is presented in the following figure (4.1.10.42). A six days period of the recording of the Earth's electric field, prior to Kythira EQ, is presented in the following figure.

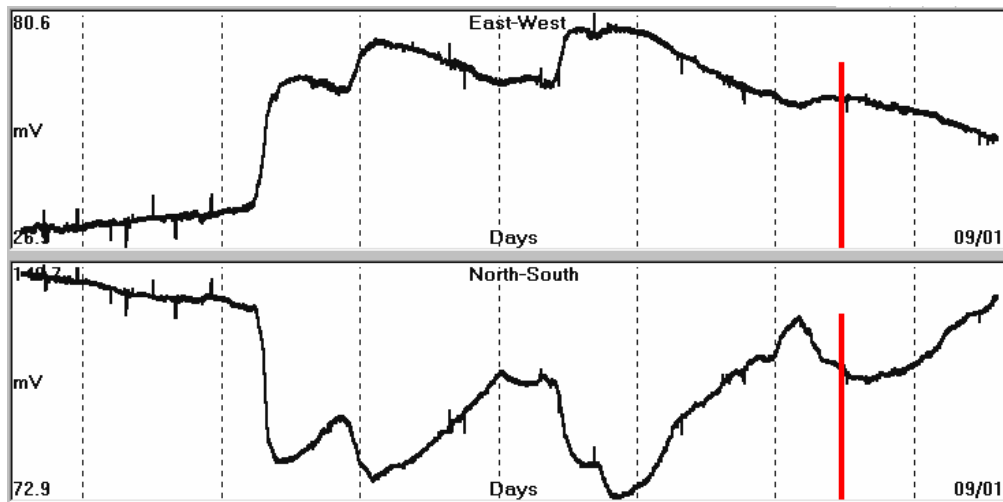


Fig. 4.1.10.42. Six (6) days recording of the Earth's electric field, recorded by **PYR** monitoring before Kythira EQ time of occurrence (red bar).

Although **VLP** signals, longer than 14 days period, have not been correlated to corresponding longer period tidal oscillations, their shorter wavelength content, is correlated very well. Actually, in terms of spectral analysis, these signals provide the appropriate oscillating components which are observed before any strong seismic event.

Generally, the **oscillating** and the **VLP** electrical signals suggest a generating mechanism which resembles, very close, the piezoelectric one or “**it behaves very closely to it**”.

So far, the tidal triggering mechanism of the earthquakes has been investigated and moreover it has been correlated to the generation of seismic, precursory, electrical signals. This has an immediate effect in the methodology, for the calculation of the timing of a strong EQ. This is demonstrated in the following figure (4.1.10.43).

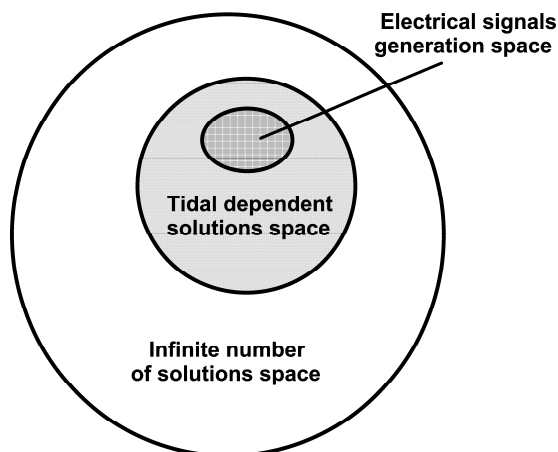


Fig. 4.1.10.43. Schematic presentation of the timing constrain of the occurrence of a strong EQ, through the use of the tidally, triggered, oscillating, lithospheric plate and the corresponding, triggered mechanisms for the generation of the preseismic, electrical signals.

The infinite number of timing solutions which result from the mass-friction model, which is generally adopted, is further strongly constrained through the use of the tidally, oscillating, lithospheric plate and the very basic theory of rock mechanics, concerning rock fracture while, finally, the short-term timing which is required for the EQ prediction, is achieved through the incorporation of the seismic, precursory electrical signals, at its final stage.

At this stage, the steps to be followed, as far as it concerns the utilization of the “short-term” time prediction of a strong EQ, are as follows:

- a. Continuous **VLP monitoring** and evaluation of any “anomalous” signal, observed.
- b. Continuous **monitoring of SES signals**. These signals indicate that “critical” strain-stress charge” conditions of the lithosphere have been reached.
- c. Continuous **monitoring of 14 days period, electrical field oscillation**, as far as it concerns their presence and amplitude increase.
- d. Continuous **monitoring of 1 - day period, electrical field oscillation**, as far as it concerns their presence and amplitude increase **in relation to the 14days period, tidal oscillation**.

The most probable time of occurrence of the pending, strong EQ will be the one that meets the criteria, already presented, in this analysis.

The increase of the daily oscillation of the Earth’s electric field, prior to the next to come 14-days period, tidal oscillation peak value, has been proved the most effective one, in terms of short-term earthquake prediction. The cases of Skyros (M=6.1) and Kythira (M=6.9) EQs are characteristic examples, for which a prediction time, with an error less than an hour (!), was estimated, always following the presented methodology.

In a real time application of the methodology, it is evident that the more the observations for analysis are available, from a widely expanded monitoring network, the better results will be achieved.

In conclusion, the time of occurrence of a strong EQ can be predicted, within a very narrow “time window” thus, justifying the use of terms of: either “short term” or “immediate” prediction.